# Dynamics of Anderson localization

# Multiple scattering of electrons

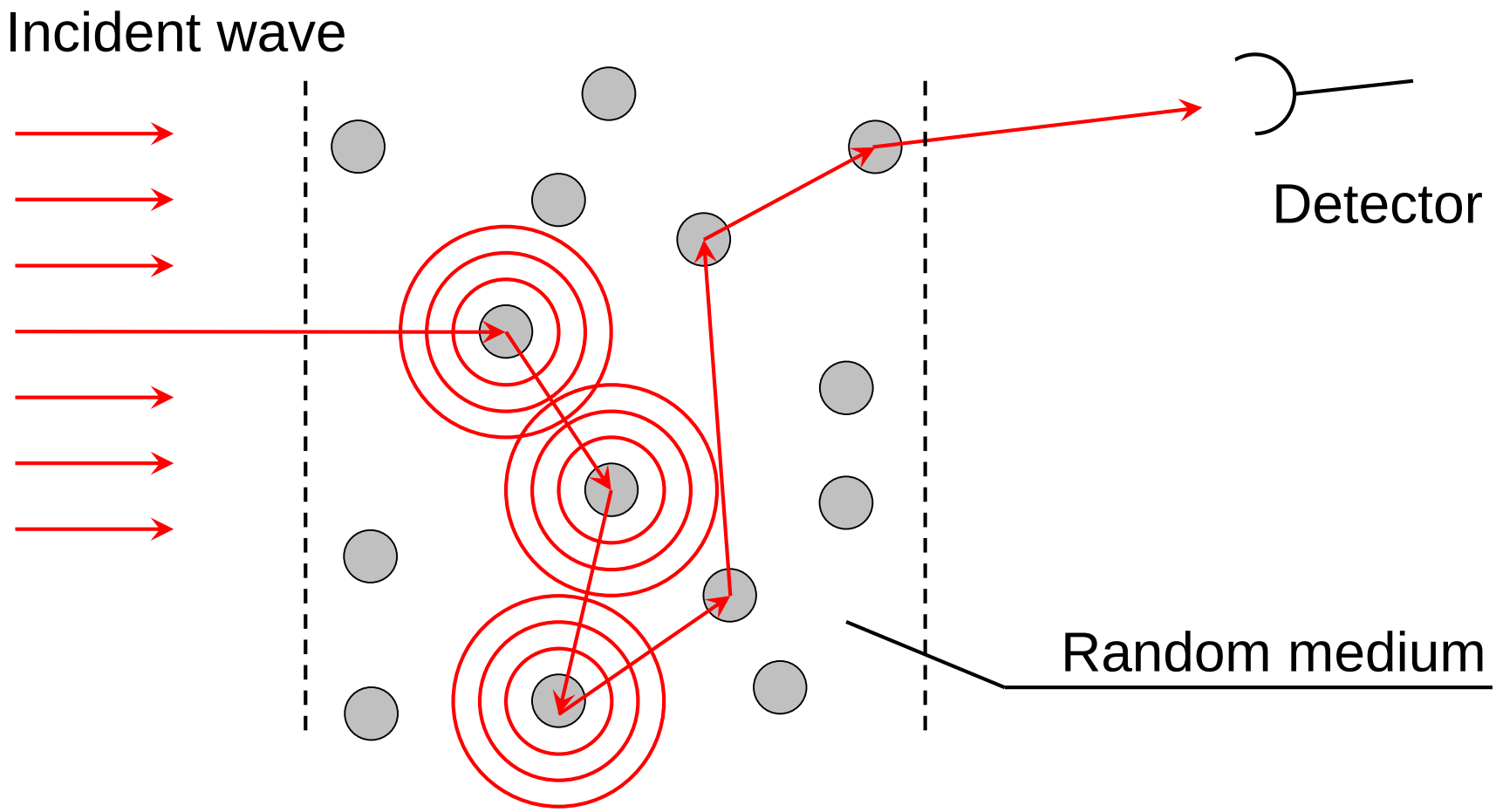

# Multiple scattering of electrons

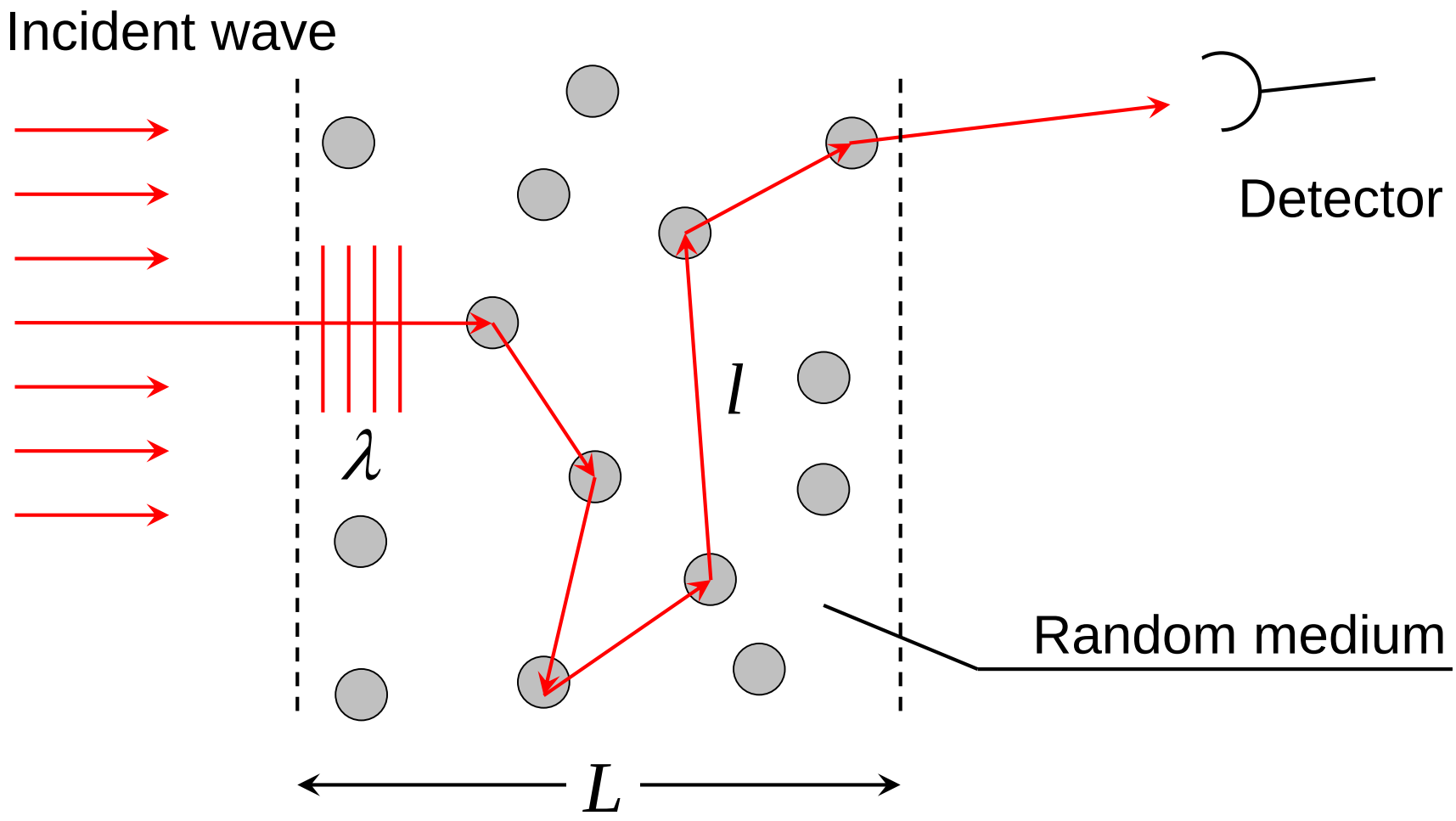

# Anderson Localization

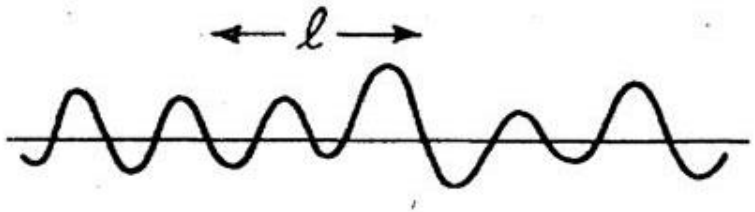


Extended state with mean free path $\ell$

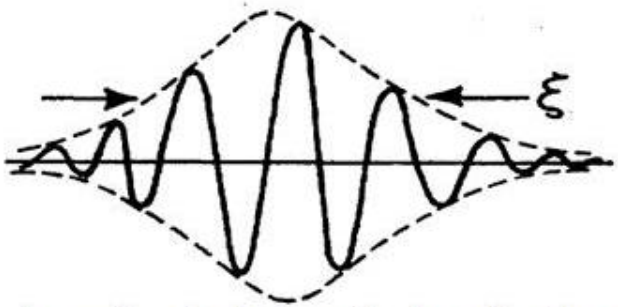


Localized state with localization length $\xi$

Lee and Ramakrishnan Rev. Mod. Phys. **57** (1985)

# Anderson localization (1957)

$$\left[-\frac{\boldsymbol{\nabla}^2}{2m} + U(\boldsymbol{r})\right]\psi_\alpha(\boldsymbol{r}) = \xi_\alpha \psi_\alpha(\boldsymbol{r})$$

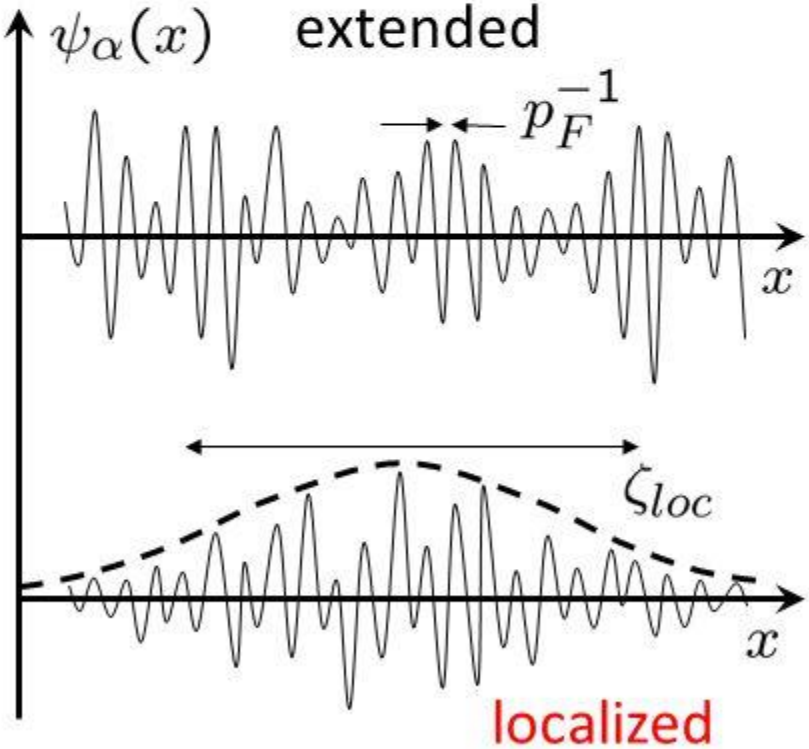


Only phase transition possible!!!

# Theoretical description of Anderson localization

- Supersymmetric nonlinear $\sigma$–model
- Random matrix theory
- Self-consistent theory of Anderson localization

---

- Lattice models
- Random walk models

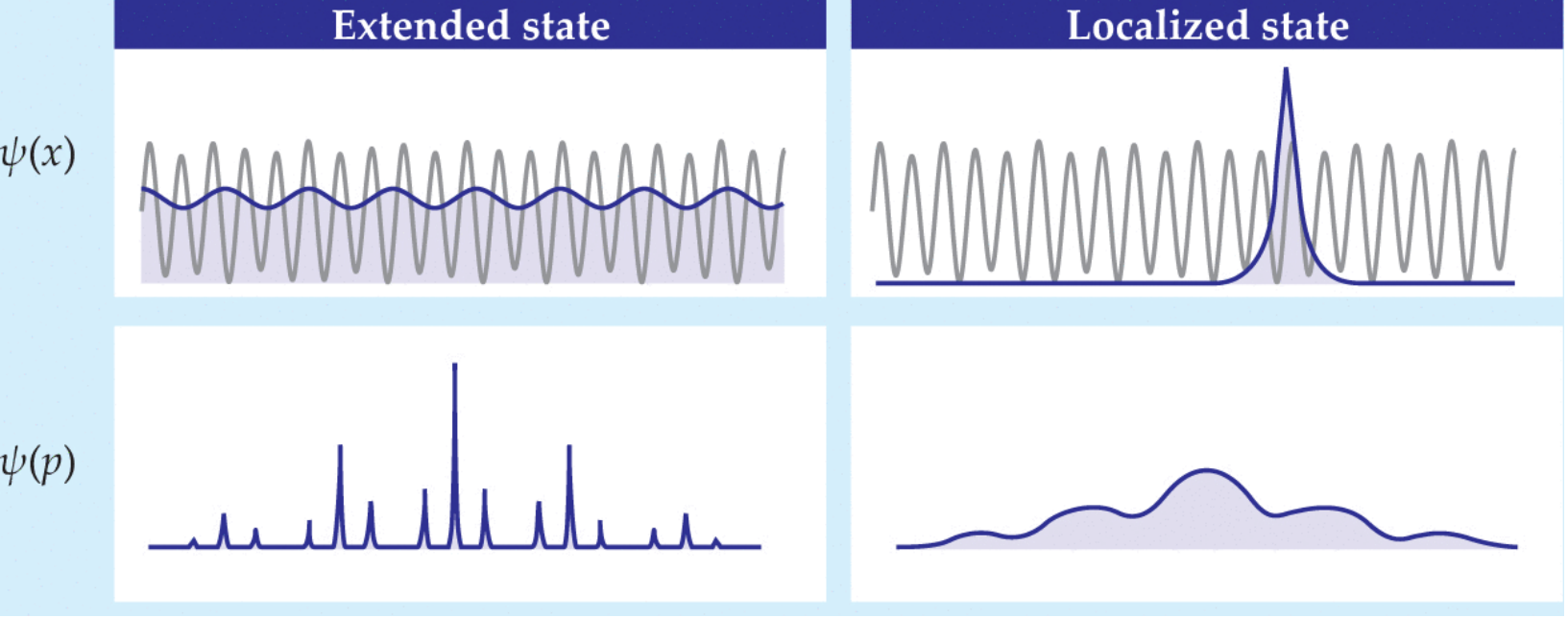
Extended state
Localized state
ψ(x)
ψ(p)

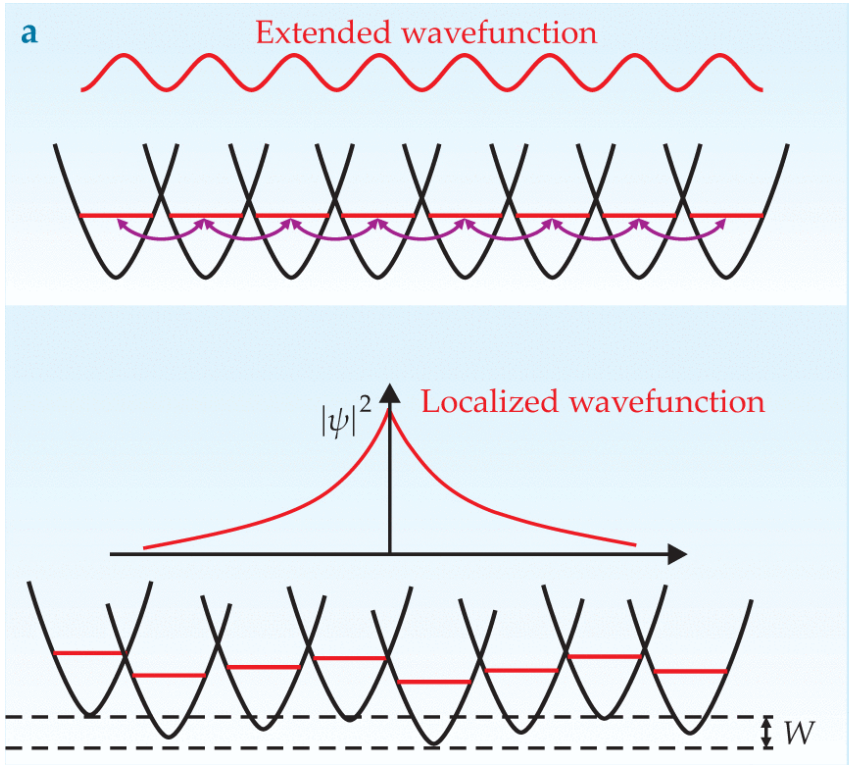
a
Extended wavefunction
|ψ|²
Localized wavefunction
W

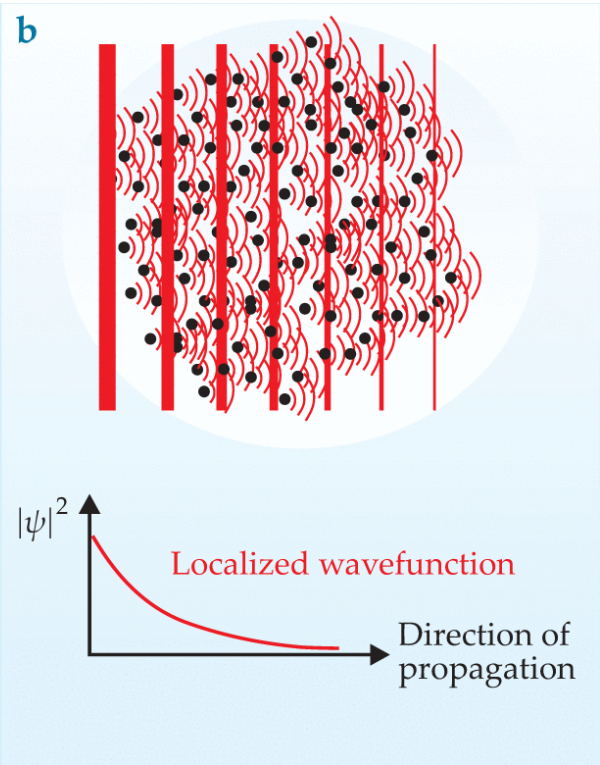
b
|ψ|²
Localized wavefunction
Direction of propagation

# From single scattering to Anderson localization

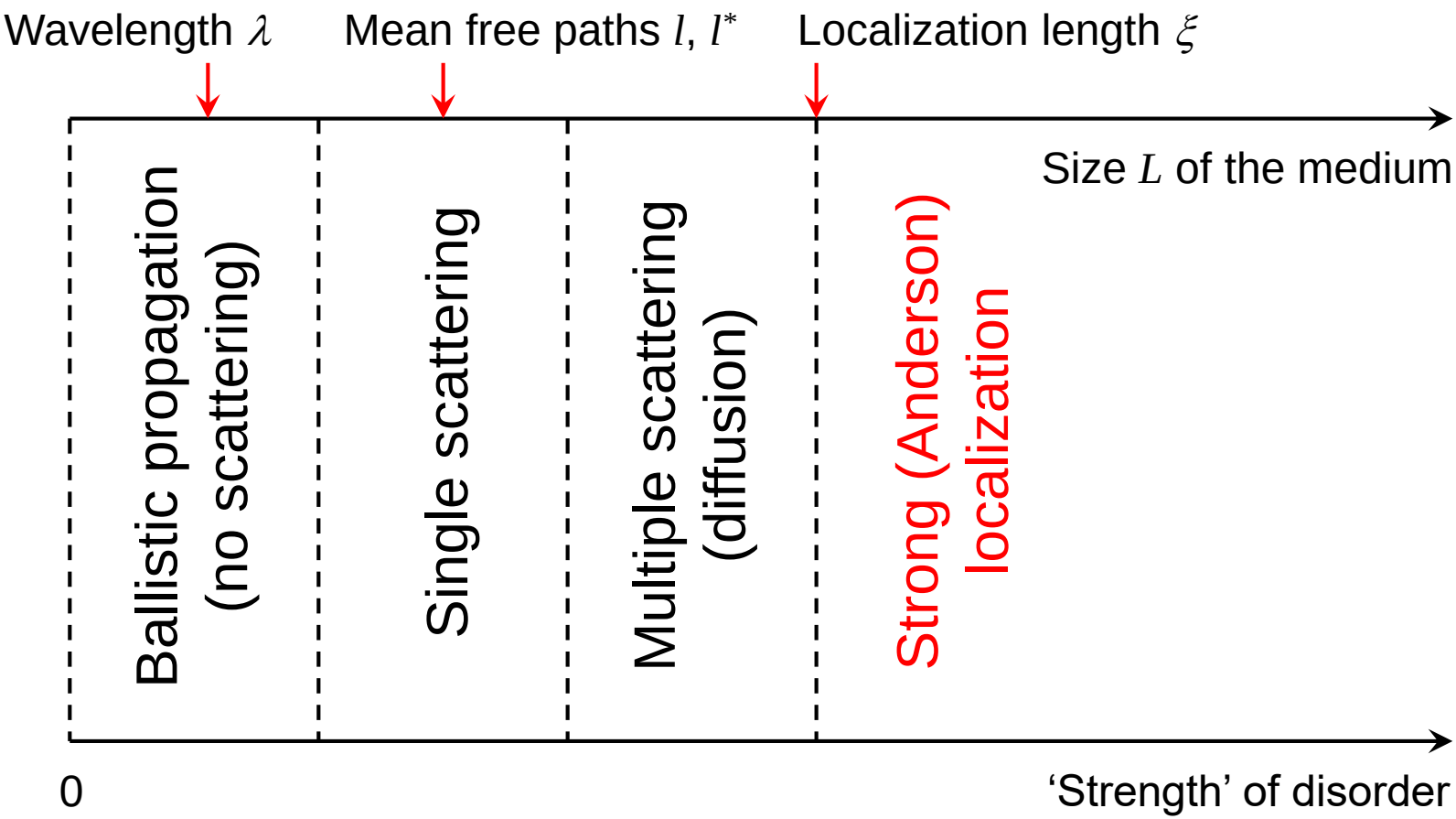

# Anderson localization of electrons: Experimental signatures

Exponential scaling of average transmission with $L$

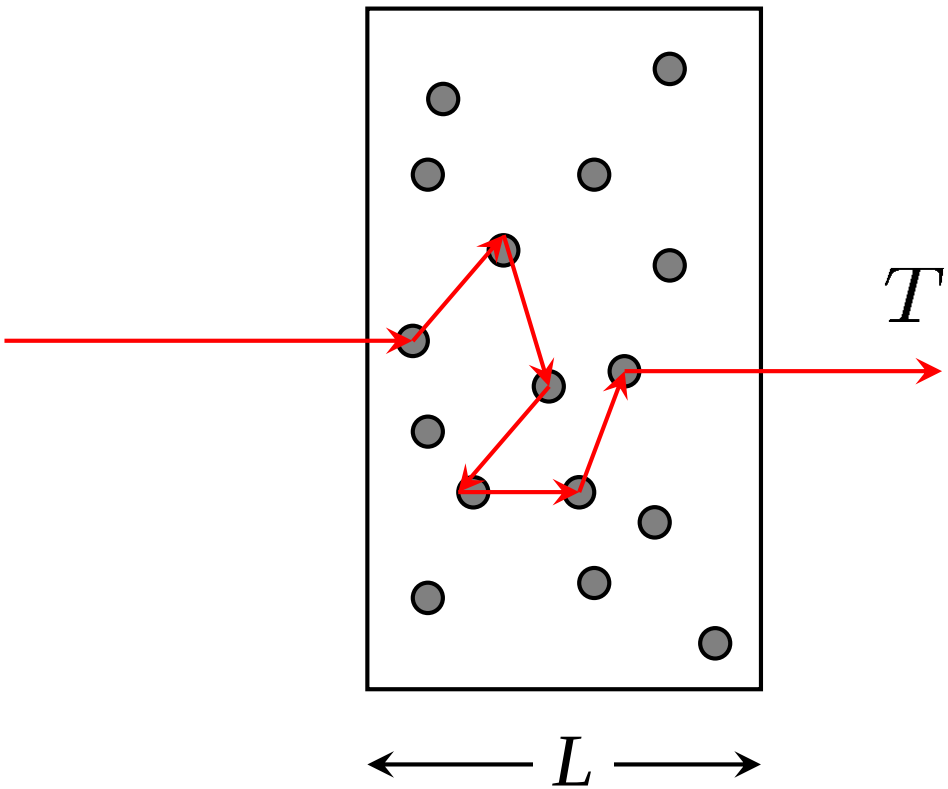


Diffuse regime:

$$\langle T \rangle \propto \frac{\ell}{L}$$

Localized regime:

$$\boxed{\langle T \rangle \propto \exp\left(-\frac{L}{\xi}\right)}$$

Measured by D.S. Wiersma *et al.*, *Nature* **390,** 671 (1997)

HOP!

# Anderson localization of electrons: Experimental signatures

## Rounding of the coherent backscattering cone

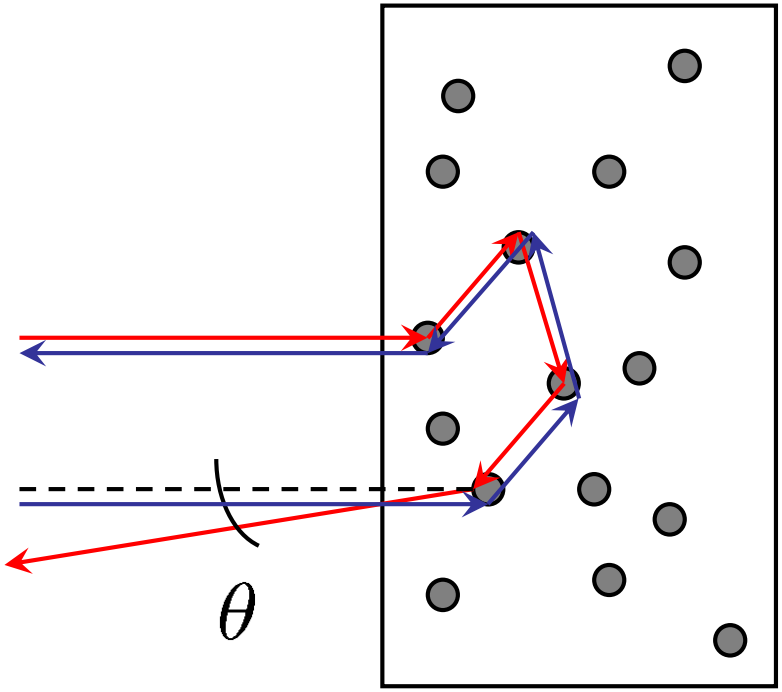


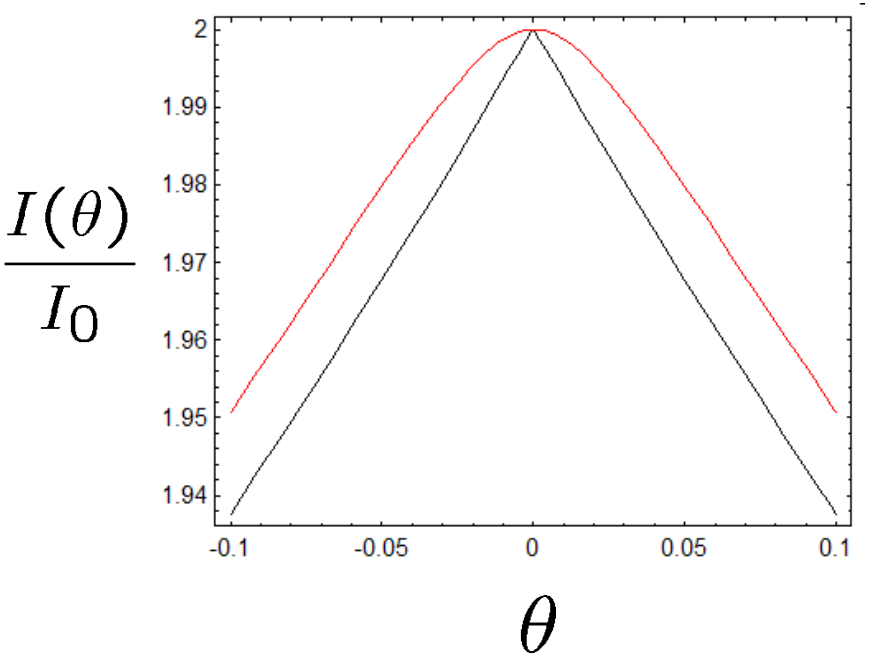


Measured by J.P. Schuurmans *et al.*, *PRL* **83,** 2183 (1999)

# Anderson localization of electrons: Experimental signatures

## Enhanced fluctuations of transmission

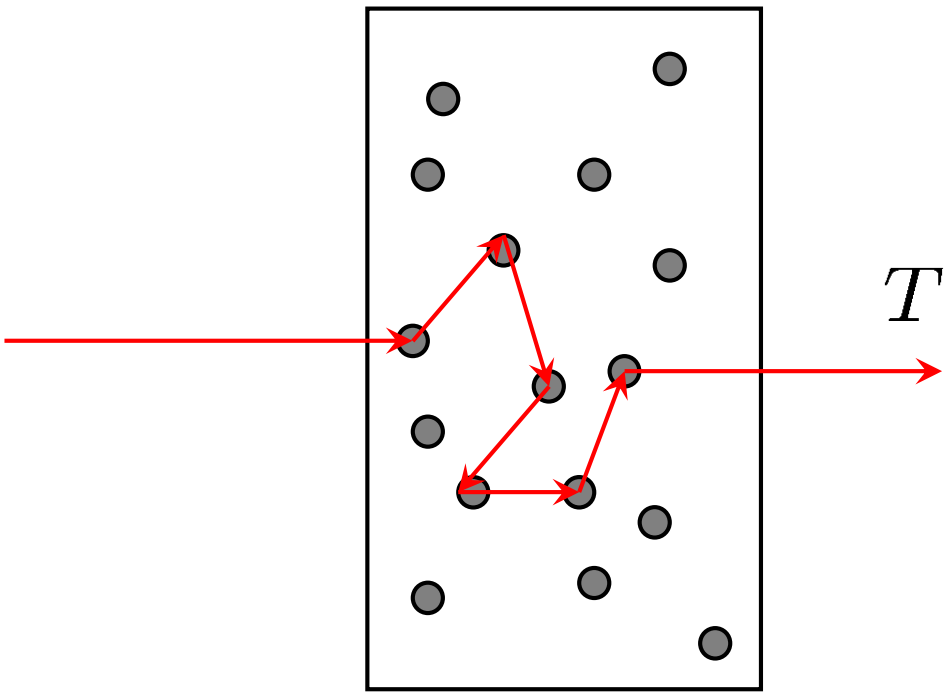


Diffuse regime:

$$\frac{\langle \delta T^2 \rangle}{\langle T \rangle^2} \ll 1$$

Localized regime:

$$\frac{\langle \delta T^2 \rangle}{\langle T \rangle^2} > const \sim 1$$

Measured by A.A. Chabanov *et al., Nature* **404,** 850 (2000)

# And what if we look in dynamics ?

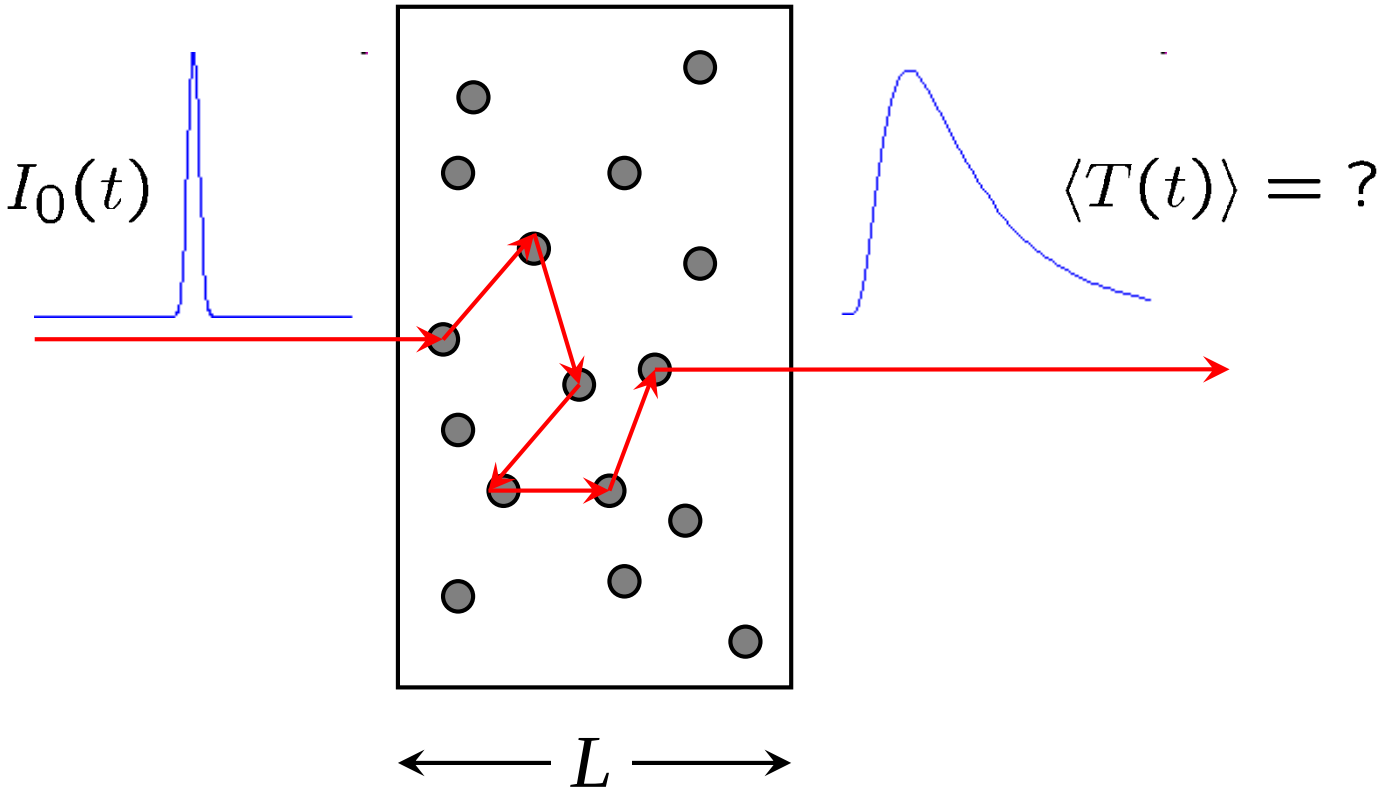

# Time-dependent transmission: diffuse regime ($L$ ⑥ ⊠)

$$\langle T(t)\rangle = -\frac{D_{\mathsf{B}}}{2\pi}\int_{-\infty}^{\infty}\frac{\partial}{\partial z}C(z=L,z'=\ell,\Omega)e^{-i\Omega t}\mathrm{d}\Omega$$

Diffusion equation

$$\left[-i\Omega - D_{\mathsf{B}}\frac{\partial^2}{\partial z^2}\right]C(z,z',\Omega) = \delta(z-z'),\;\; D_{\mathsf{B}} = \frac{v_{\mathsf{E}}\ell}{3}$$

+

Boundary conditions

$$C(z,z',\Omega) \mp z_0\frac{\partial}{\partial z}C(z,z',\Omega) = 0,\quad z=0,L,\quad z_0\sim\ell$$

# Time-dependent transmission: diffuse regime ($L$ ⑥ ⊠)

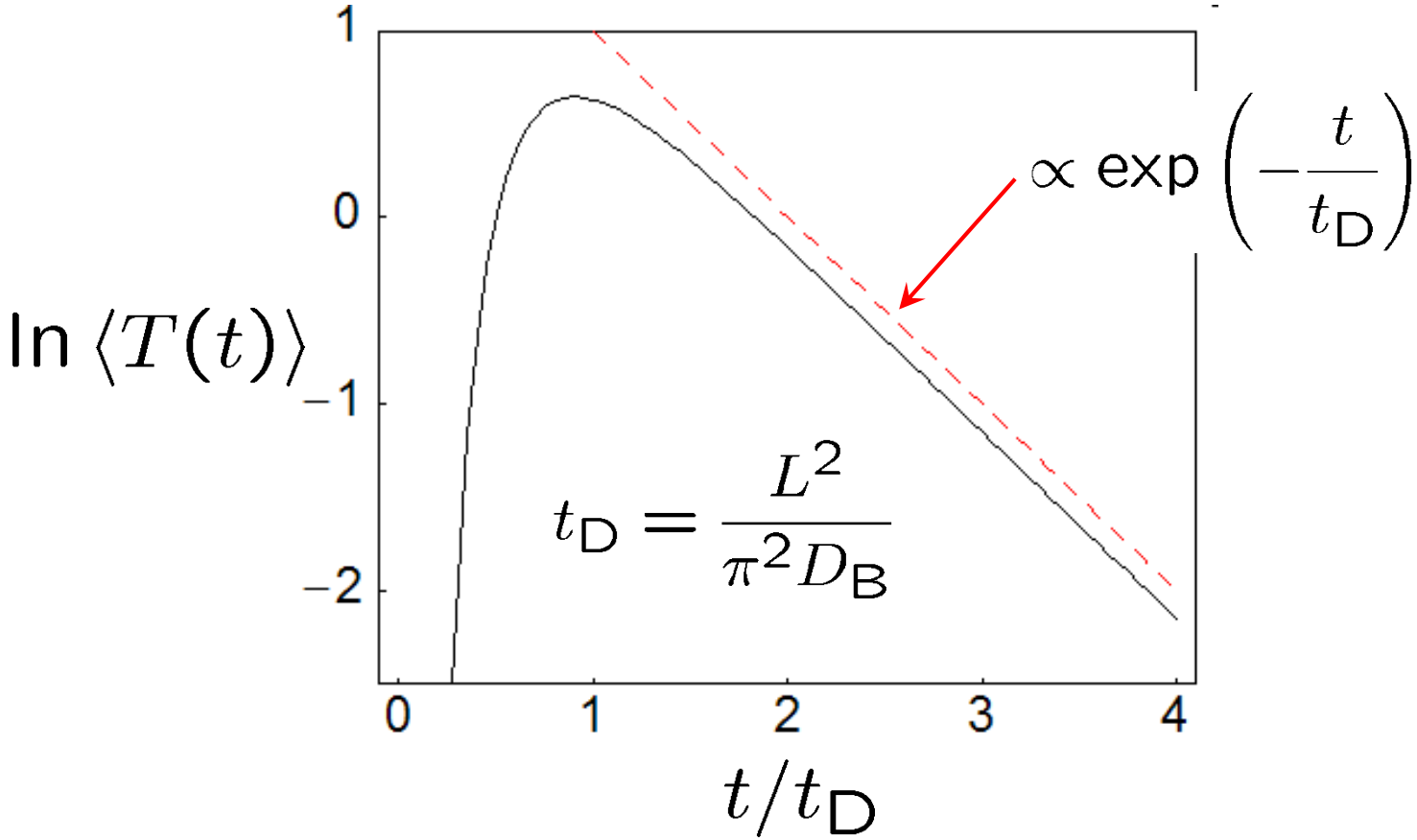


How will $\langle T(t) \rangle$ be modified when localization is approached ?

# Theoretical description of Anderson localization

- Supersymmetric nonlinear $\sigma$–model
- Random matrix theory
- Self-consistent theory of Anderson localization

---

- Lattice models
- Random walk models

# Self-consistent theory of Anderson localization

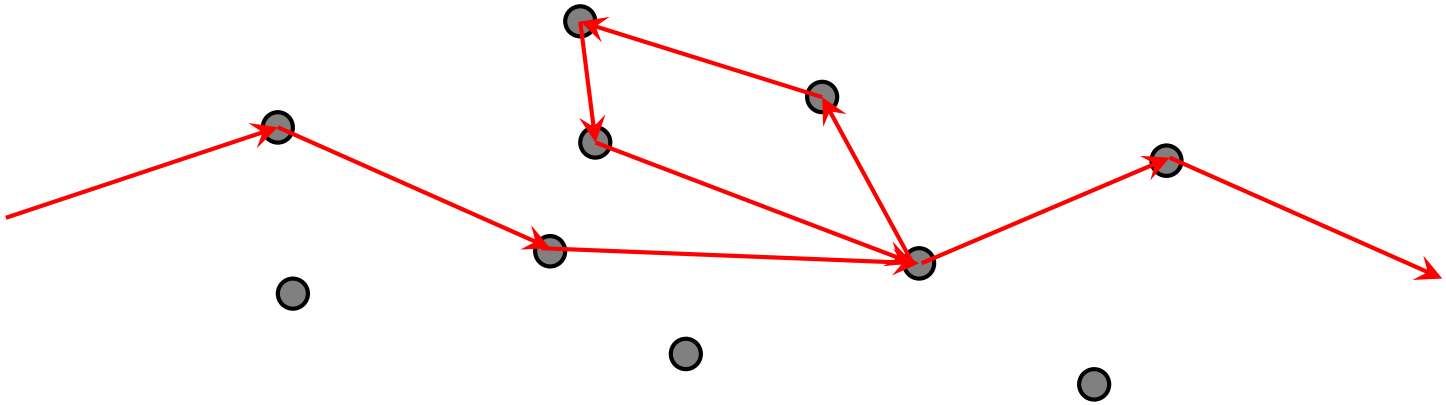

# Self-consistent theory of Anderson localization

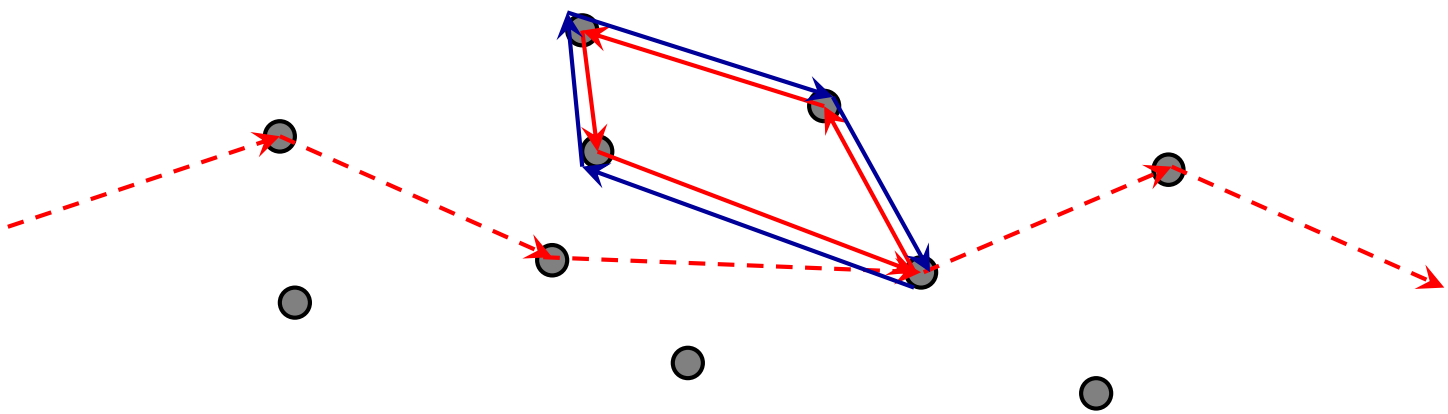

The presence of loops increases return probability as compared to ‘normal’ diffusion

⇩

Diffusion slows down

⇩

Diffusion constant should be renormalized $D_{\mathrm{B}} \to D < D_{\mathrm{B}}$

# Generalization to open media

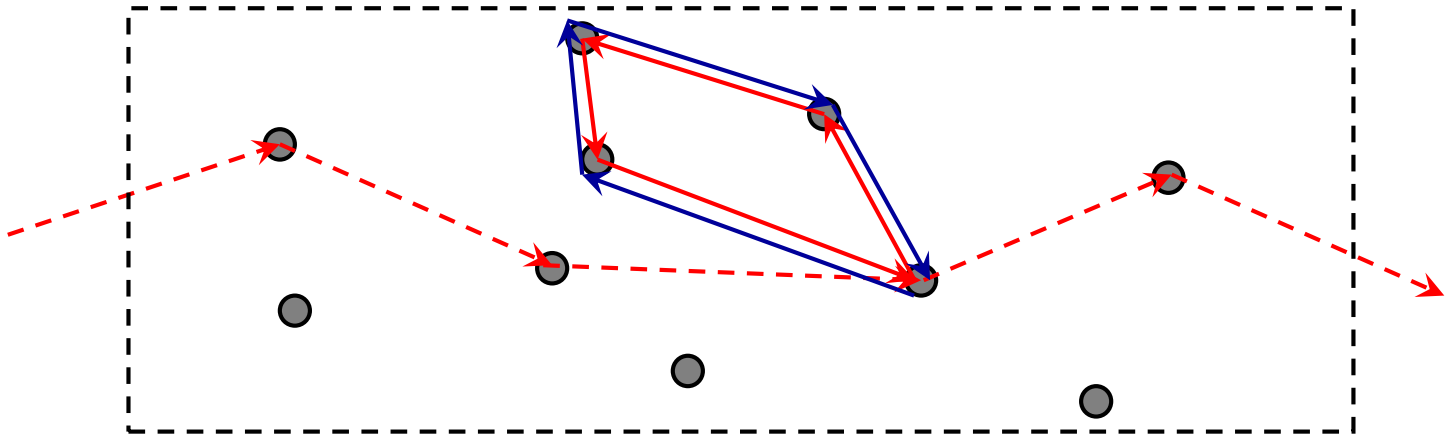

Loops are less probable near the boundaries

Slowing down of diffusion is spatially heterogeneous

Diffusion constant becomes position-dependent

$$D_{\mathrm{B}} \to D(\mathbf{r}) < D_{\mathrm{B}}$$

# Quasi-1D disordered waveguide

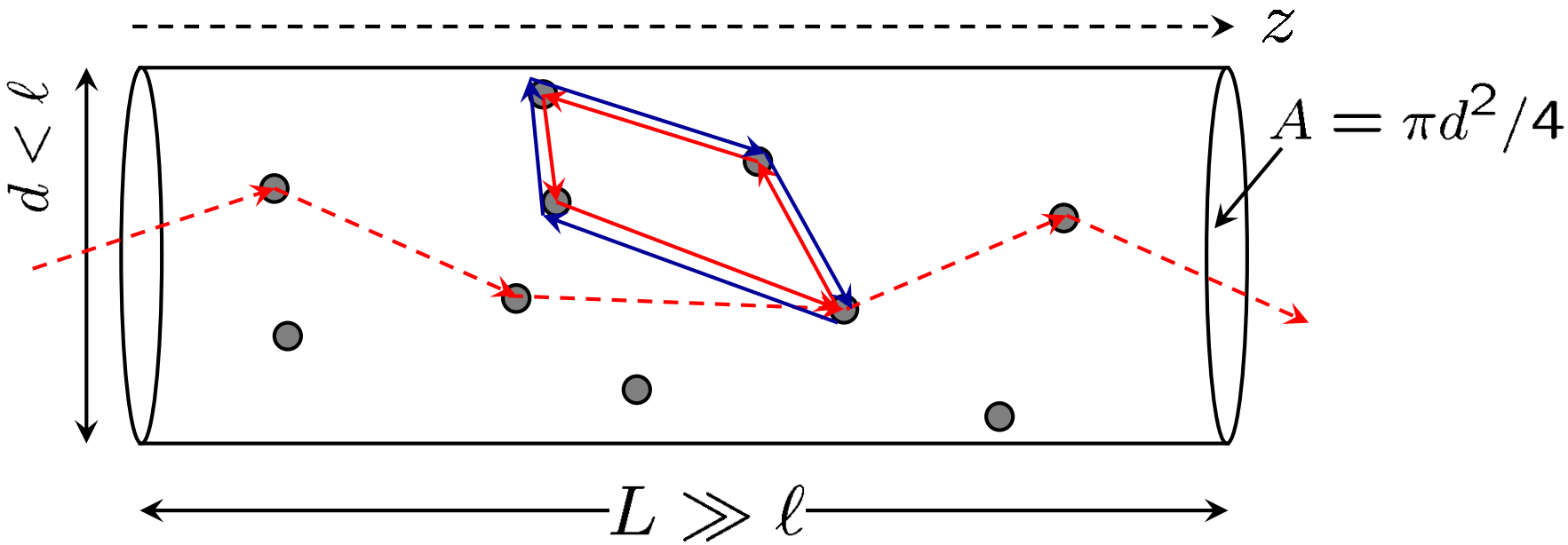


Number of transverse modes: $N = k^2 A/(4\pi)$

Dimensionless conductance: $g = (4/3)N\ell/L$

Localization length: $\xi = (2/3)N\ell$

# Mathematical formulation

Diffusion equation

$$\left[-i\Omega - \frac{\partial}{\partial z} D(z,\Omega) \frac{\partial}{\partial z}\right] C(z,z',\Omega) = \delta(z-z')$$

+

Self-consistency condition

$$\frac{1}{D(z,\Omega)} = \frac{1}{D_{\mathrm{B}}} + \frac{2}{\xi} C(z,z,\Omega)$$

+

Boundary conditions

$$C(z,z',\Omega) \mp z_0 \left[\frac{D(z,\Omega)}{D_B}\right] \frac{\partial}{\partial z} C(z,z',\Omega) = 0, \quad z = 0, L$$

# Stationary transmission: $\Omega = 0$

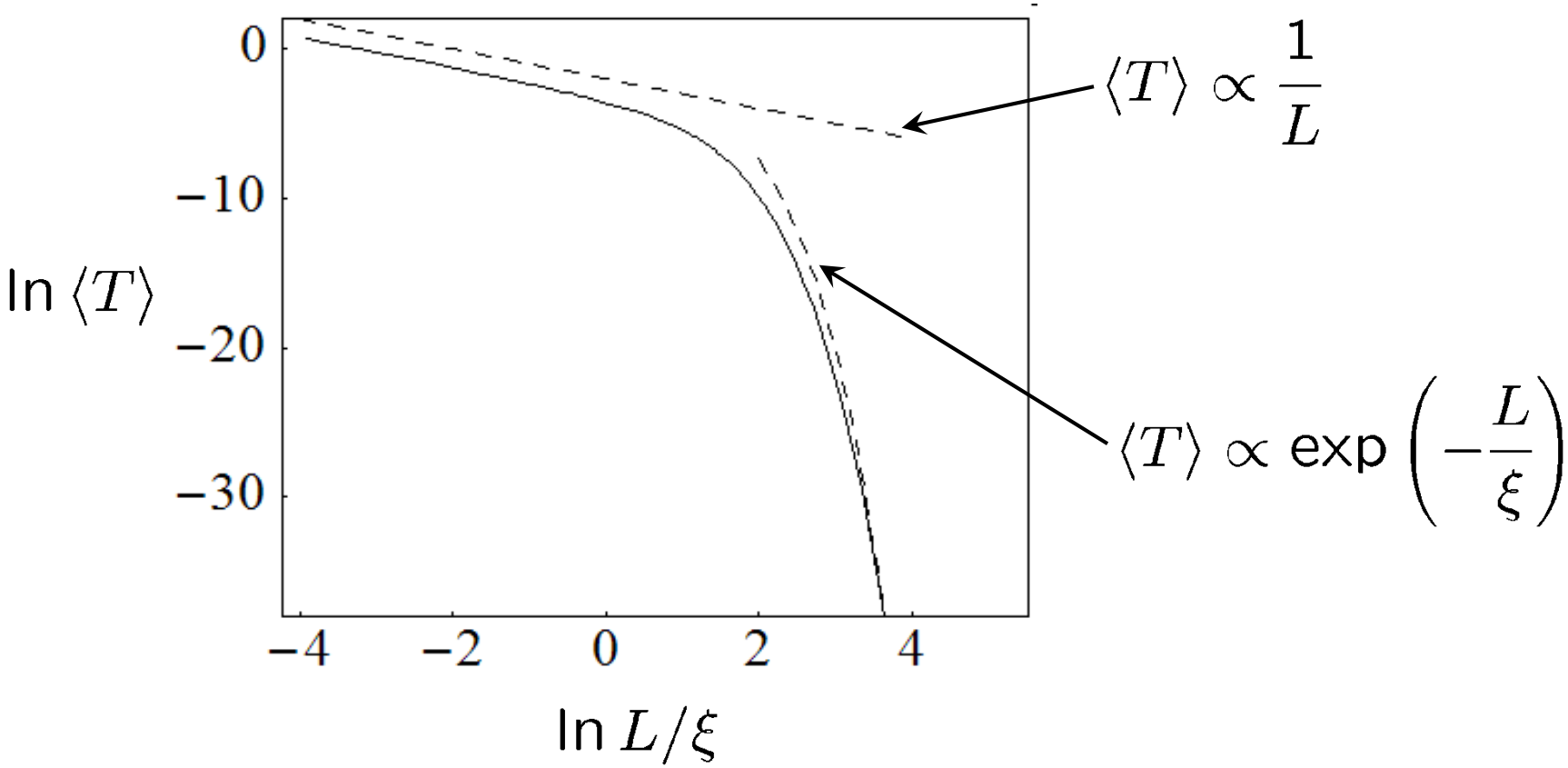

# ‘Normal’ diffusion: *g* ✹ ◎

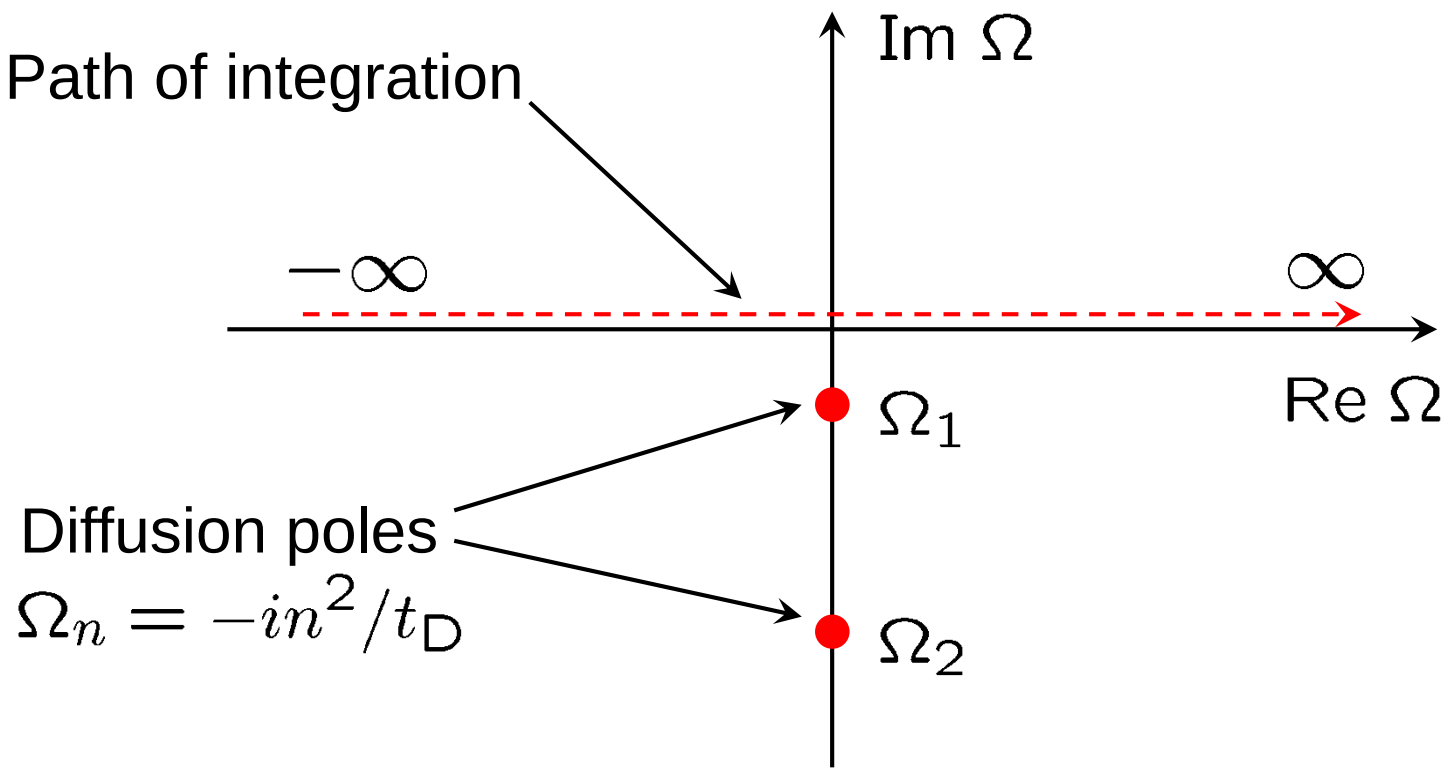


$$\Omega_n = -in^2/t_{\mathsf{D}}$$

$$\langle T(t)\rangle = -\frac{D_{\mathsf{B}}}{2\pi}\int_{-\infty}^{\infty}\frac{\partial}{\partial z}C(z=L,z'=\ell,\Omega)e^{-i\Omega t}\mathrm{d}\Omega$$

# ‘Normal’ diffusion: *g* ✸ ◎

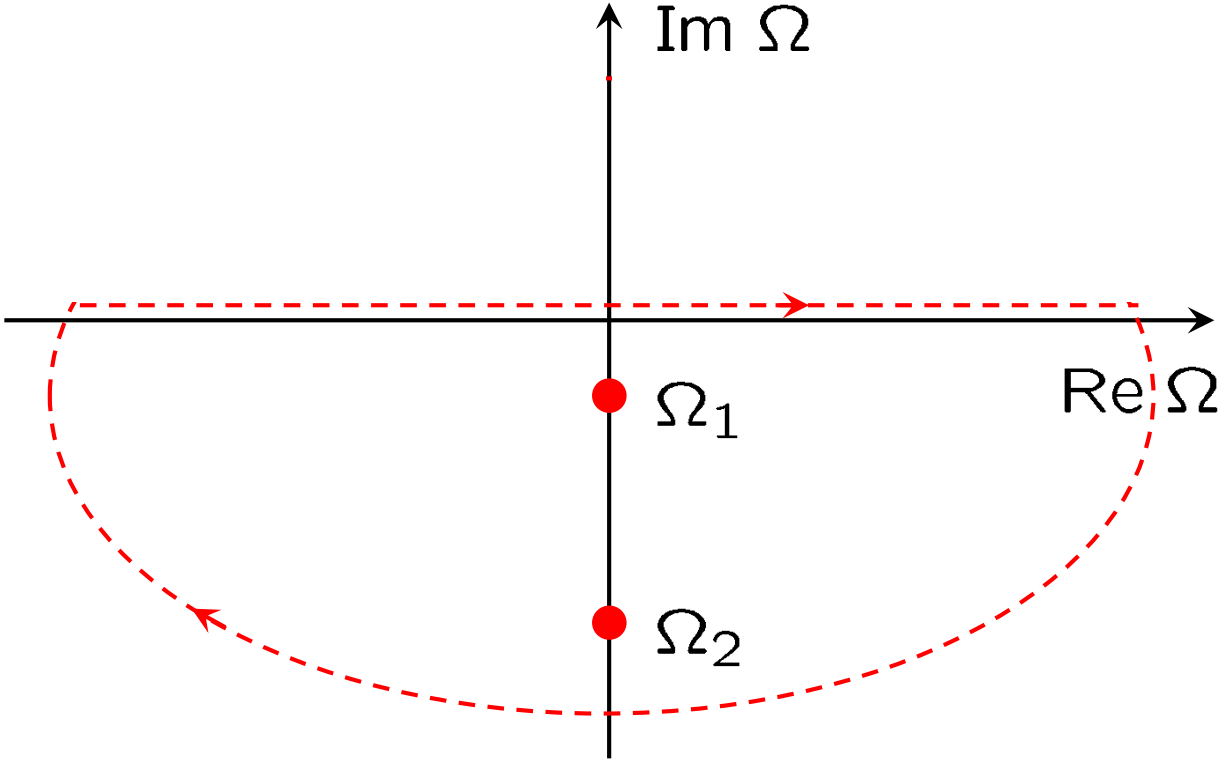


$$\langle T(t)\rangle = iD_{\mathrm{B}} \sum_{n=1}^{\infty} \mathrm{Res}\left[\frac{\partial C}{\partial z} e^{-i\Omega t}, \Omega = \Omega_n\right]$$

# ‘Normal’ diffusion: *g* ✸ ◎

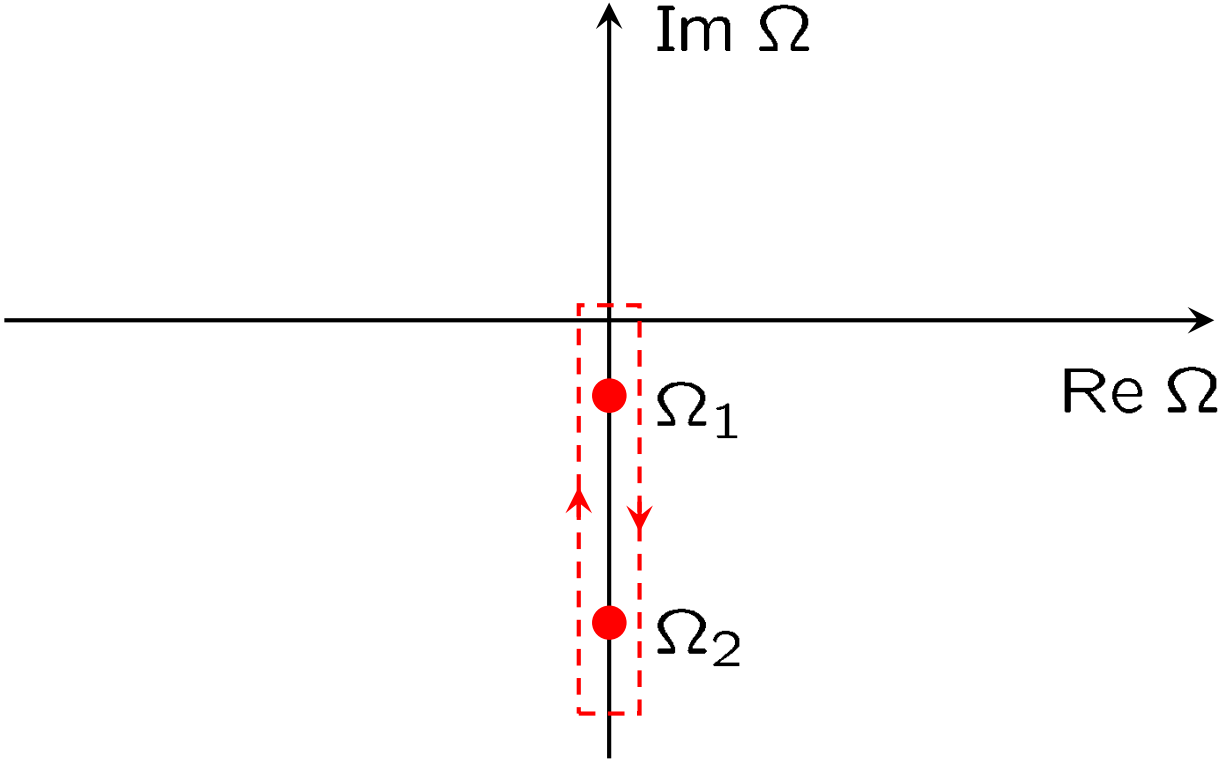


$$\langle T(t)\rangle = iD_{\mathrm{B}} \sum_{n=1}^{\infty} \mathrm{Res}\left[\frac{\partial C}{\partial z} e^{-i\Omega t}, \Omega = \Omega_n\right]$$

# From poles to branch cuts: *g* 🖫 ◎

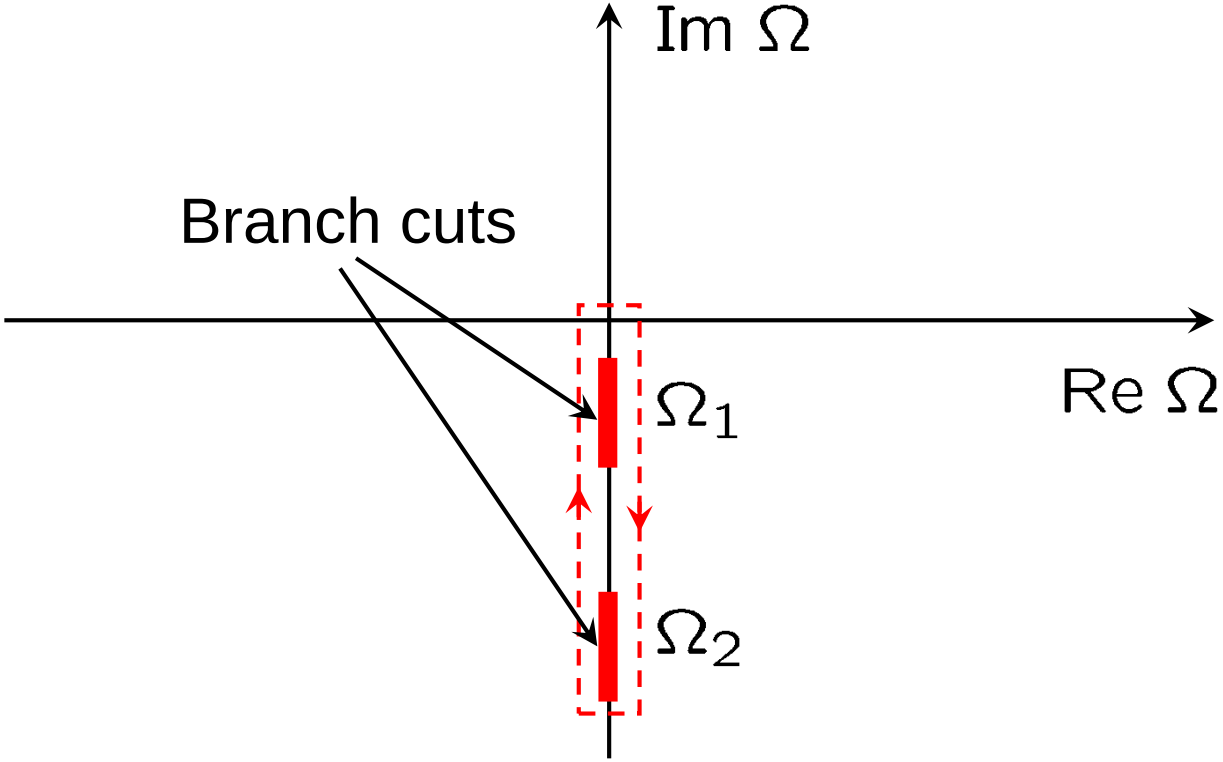


$$\langle T(t)\rangle = \int_0^\infty P_{\mathsf{T}}(\alpha) e^{-\alpha t} \mathrm{d}\alpha$$

$$P_{\mathsf{T}}(\alpha) = -i \lim_{\epsilon \to +0} \left[ D \frac{\partial}{\partial z} C(-i\alpha + \epsilon) - D \frac{\partial}{\partial z} C(-i\alpha - \epsilon) \right]$$

# Leakage function $P_{\mathrm{T}}(\text{♋})$

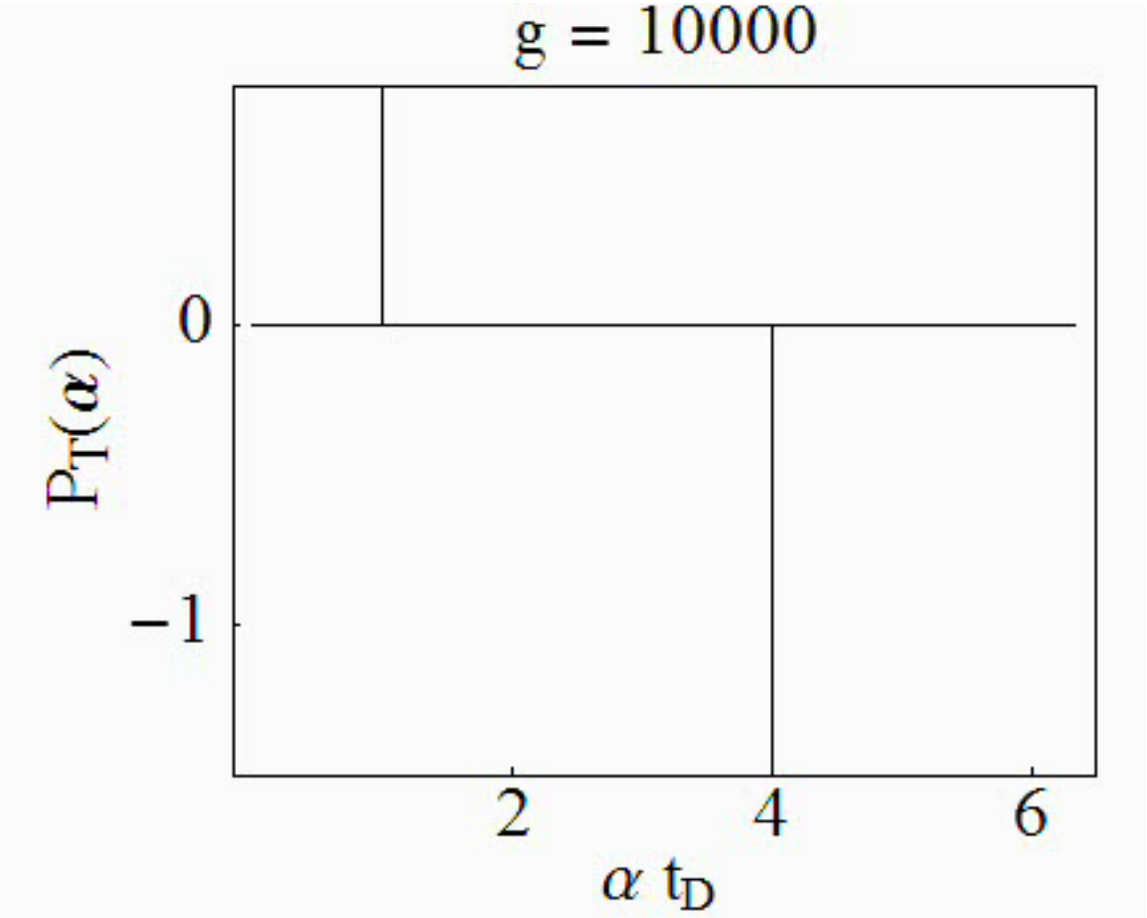

# Time-dependent diffusion constant

$$\langle T(t)\rangle \propto \exp\left[-\frac{1}{D_{\mathsf{B}} t_{\mathsf{D}}}\int_0^t \mathrm{d}t' D(t')\right]$$

$$\boxed{D(t) = -D_{\mathsf{B}} t_{\mathsf{D}} \frac{\partial}{\partial t} \ln \langle T(t)\rangle}$$

Diffuse regime: $g \gg 1, \quad D(t) = D_{\mathsf{B}}$ for $t > t_{\mathsf{D}}$

Closeness of localized regime is manifested by $\underline{D(t) < D_{\mathsf{B}}}$

# Time-dependent diffusion constant

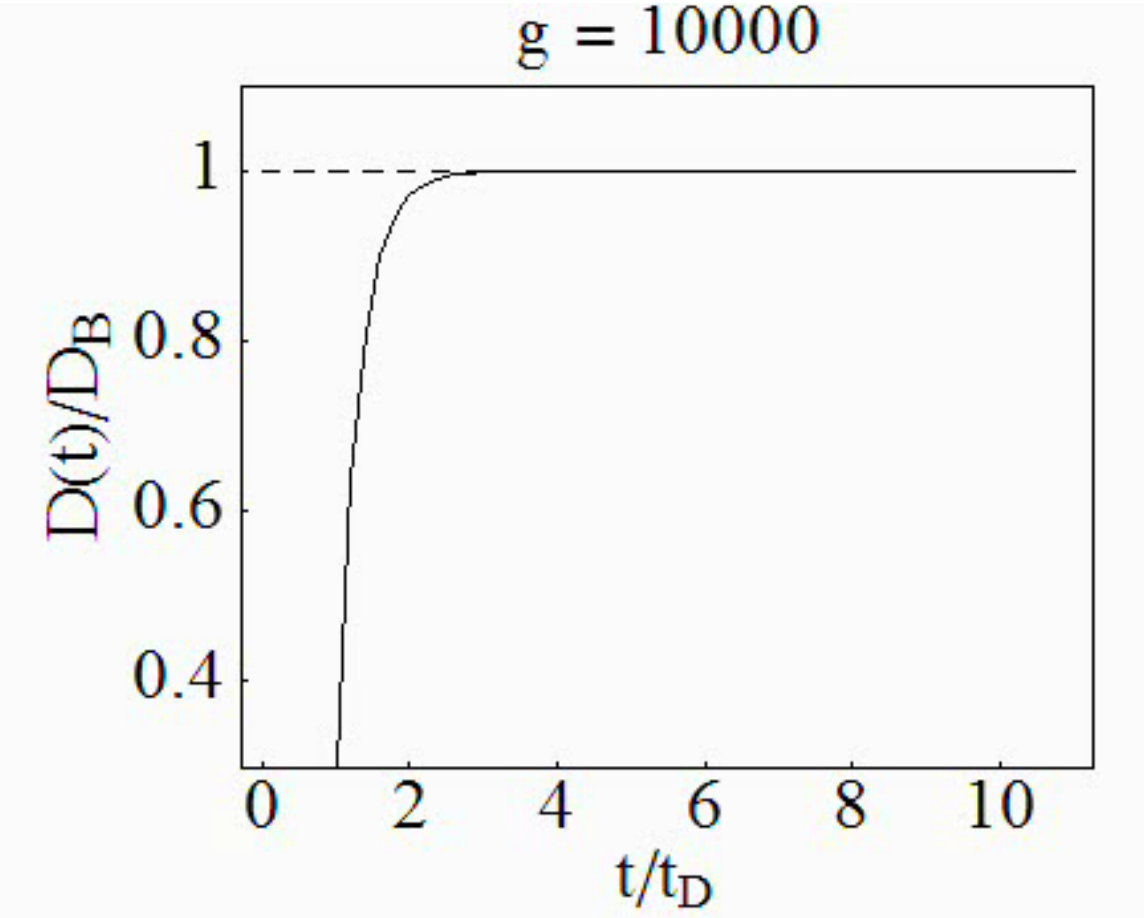

# Time-dependent diffusion constant

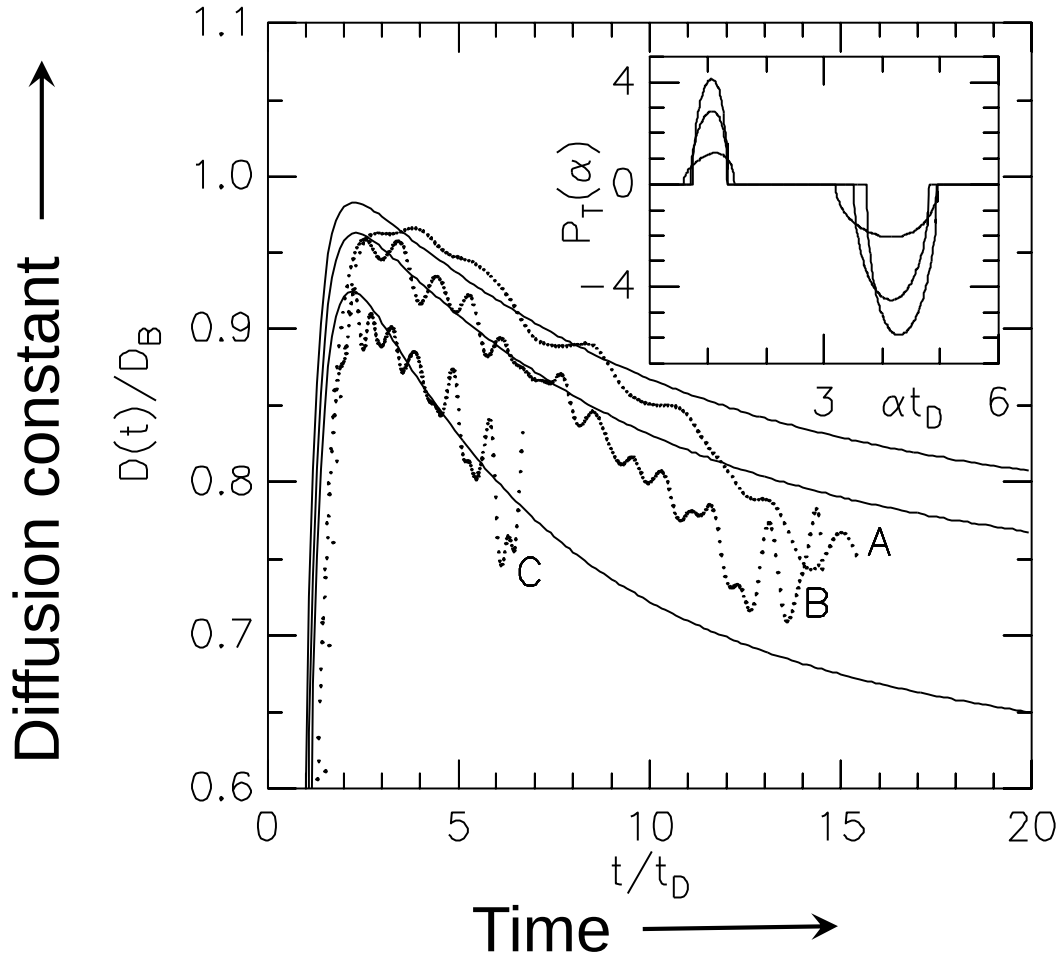


Data by A.A. Chabanov *et al. PRL* **90,** 203903 (2003)

# Time-dependent diffusion constant

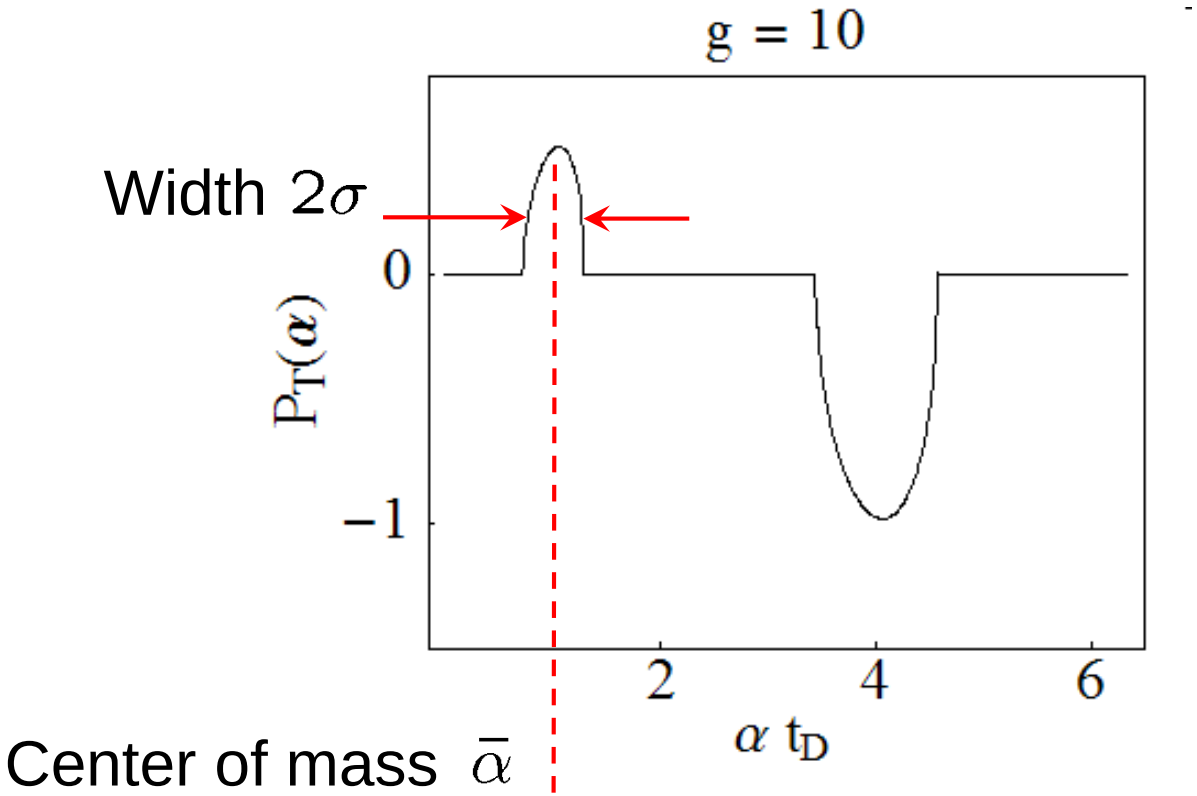


$$P_T(\alpha) \propto \exp\left[-\frac{(\alpha-\bar{\alpha})^2}{2\sigma^2}\right] \Rightarrow \frac{D(t)}{D_B} = \bar{\alpha} t_D - \sigma^2 t_D t$$

# Time-dependent diffusion constant

$$\bar{\alpha} t_{\mathsf{D}} - 1 \propto \frac{1}{g} \qquad \sigma^2 t_{\mathsf{D}}^2 \propto \frac{1}{g}$$

$$\Downarrow$$

$$\boxed{\frac{D(t)}{D_{\mathsf{B}}} = 1 + \frac{A}{g} - \frac{B}{g}\frac{t}{t_{\mathsf{D}}}}$$

$$A = \frac{3}{2\pi^2} \qquad B = \frac{2}{\pi^2}$$

Consistent with supersymmetric nonlinear $\sigma$-model
[A.D. Mirlin, *Phys. Rep.* **326,** 259 (2000)] for $t < g t_{\mathsf{D}} = t_{\mathsf{H}}$

# Breakdown of the theory for $t > t_{\mathrm{H}}$
# Mode picture

Diffuse regime: $\Delta \ll \delta$

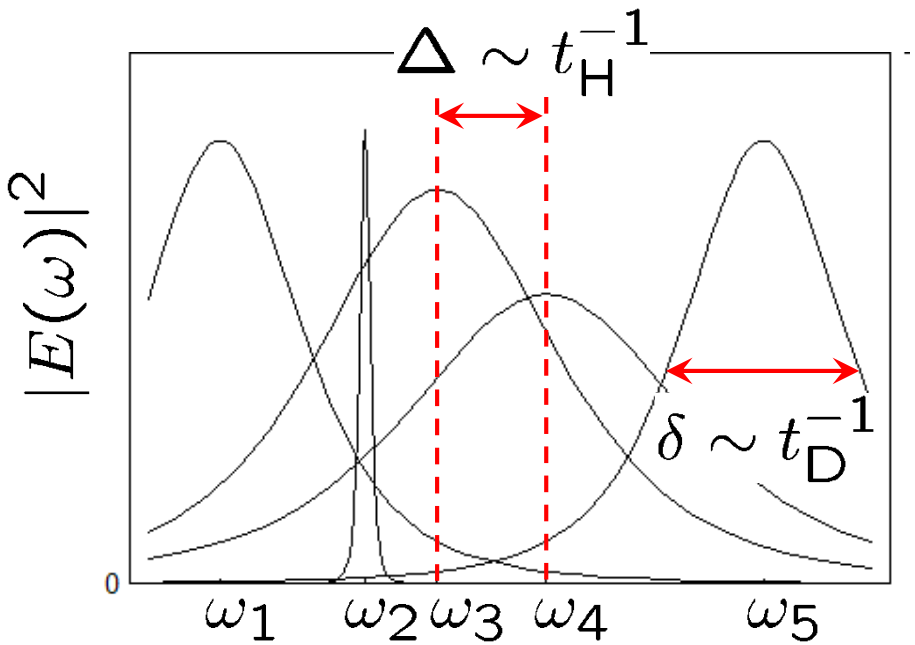


$t < t_{\mathrm{H}}$

# Breakdown of the theory for $t > t_{\mathrm{H}}$
# Mode picture

Diffuse regime: $\Delta \ll \delta$

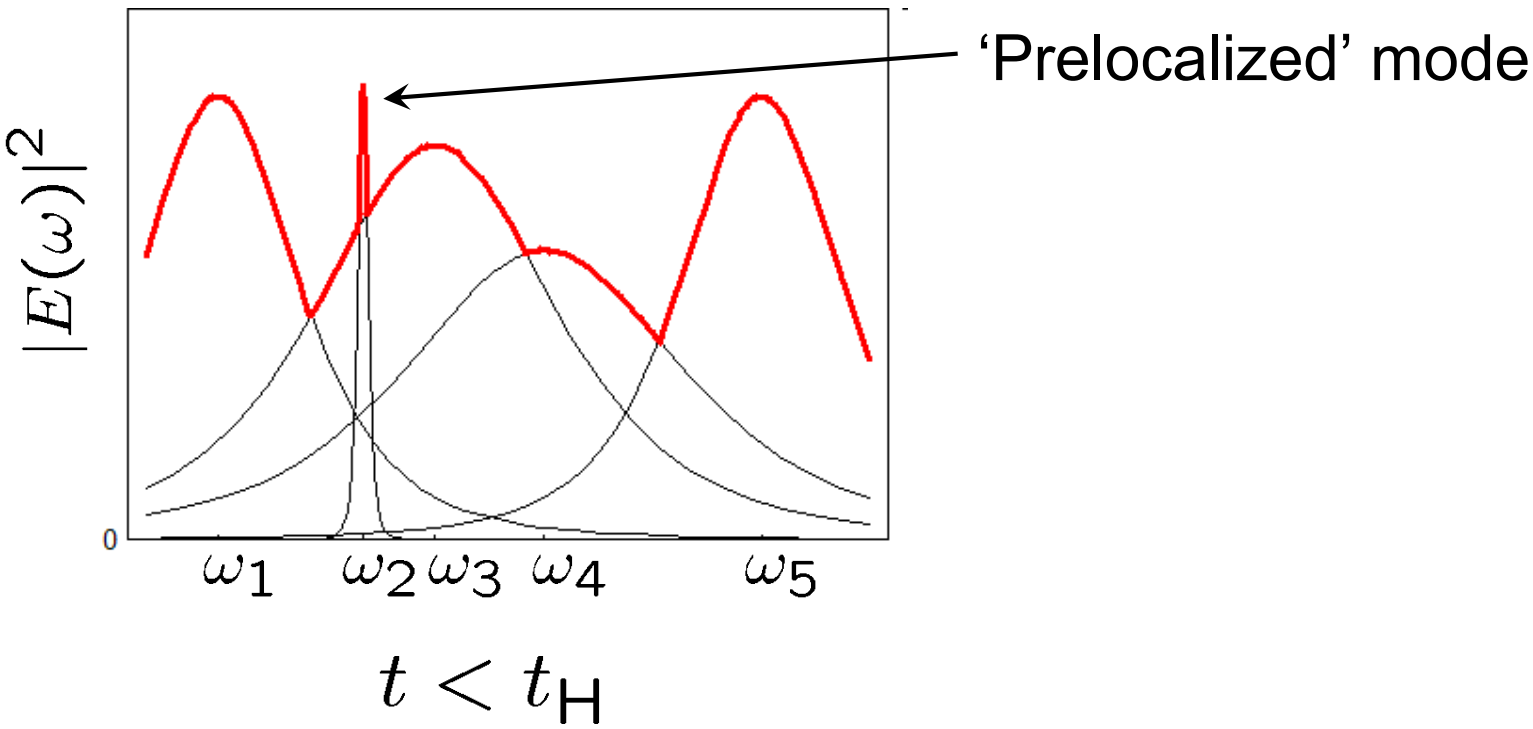


The spectrum is continuous

# Breakdown of the theory for $t > t_{\mathrm{H}}$
# Mode picture

Diffuse regime: $\Delta \ll \delta$

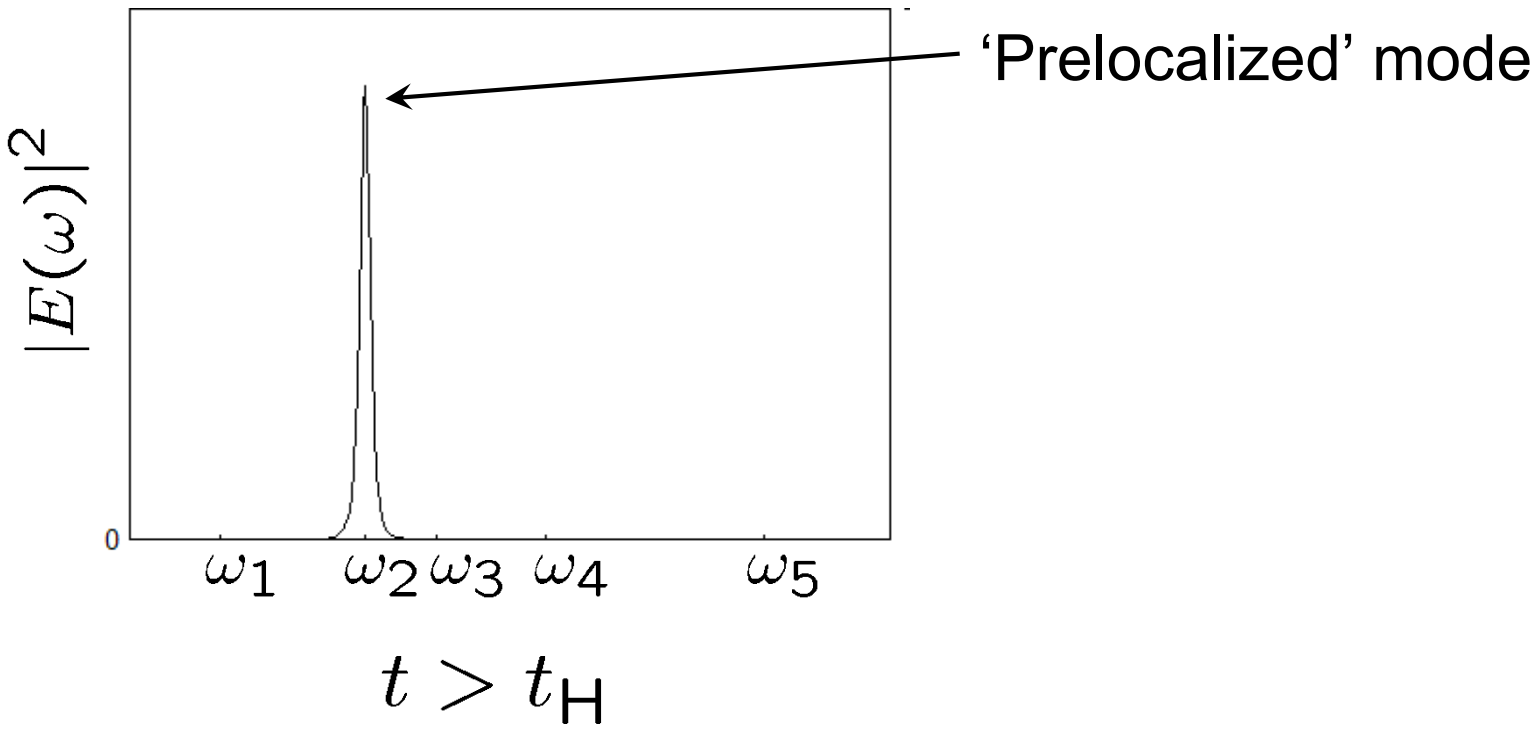


Only the narrowest mode survives

# Breakdown of the theory for $t > t_{\mathrm{H}}$
# Mode picture

Diffuse regime: $\Delta \ll \delta$

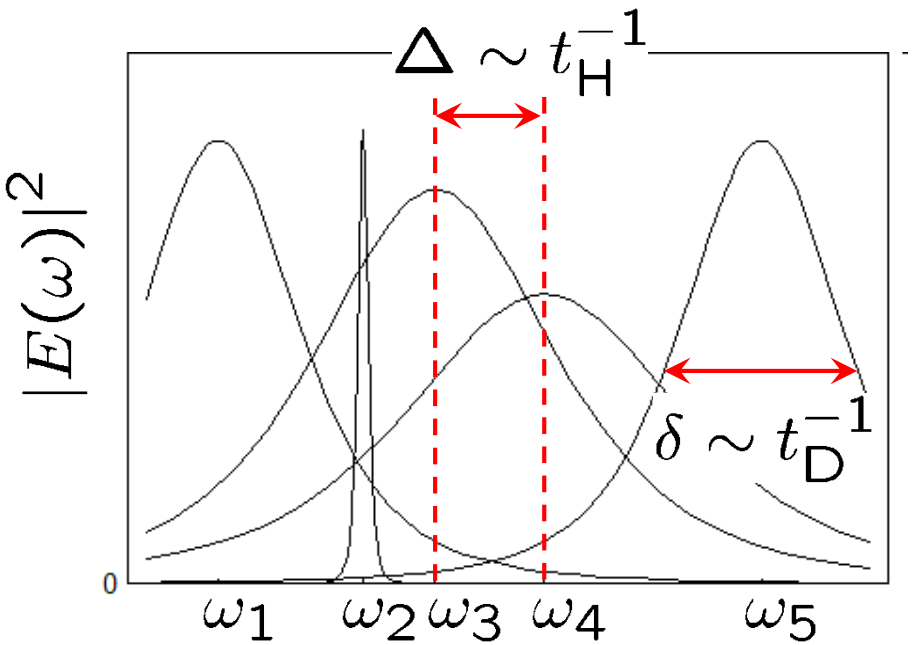


$t < t_{\mathrm{H}}$

The spectrum is continuous

Localized regime: $\Delta \gg \delta$

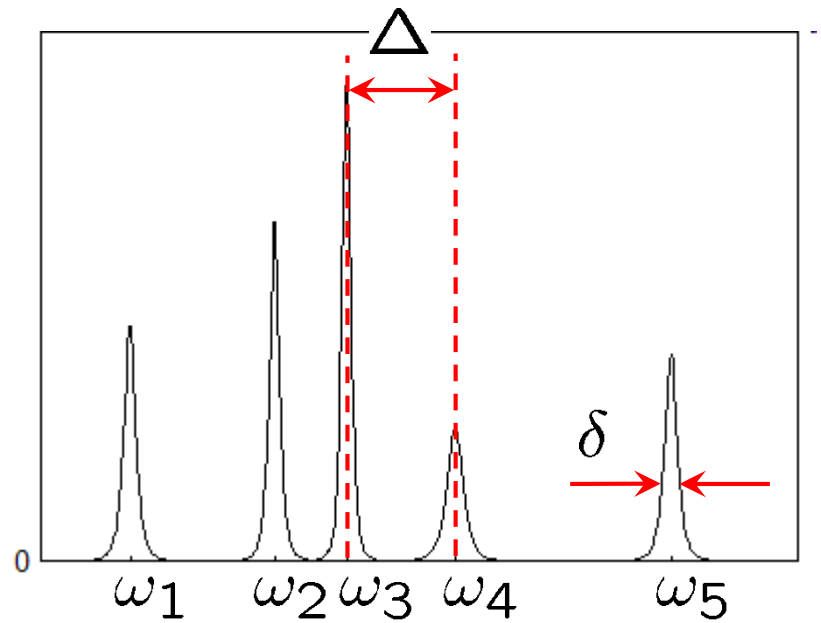


$t < t_{\mathrm{H}}$

There are many modes

# Breakdown of the theory for $t > t_{\mathrm{H}}$
# Mode picture

Diffuse regime: $\Delta \ll \delta$

Localized regime: $\Delta \gg \delta$

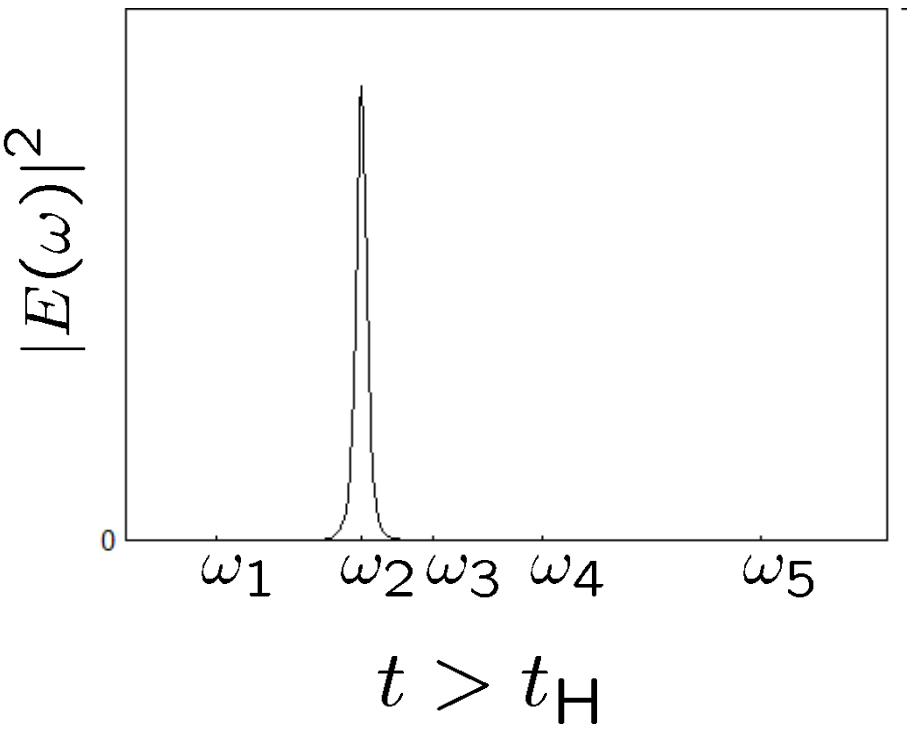


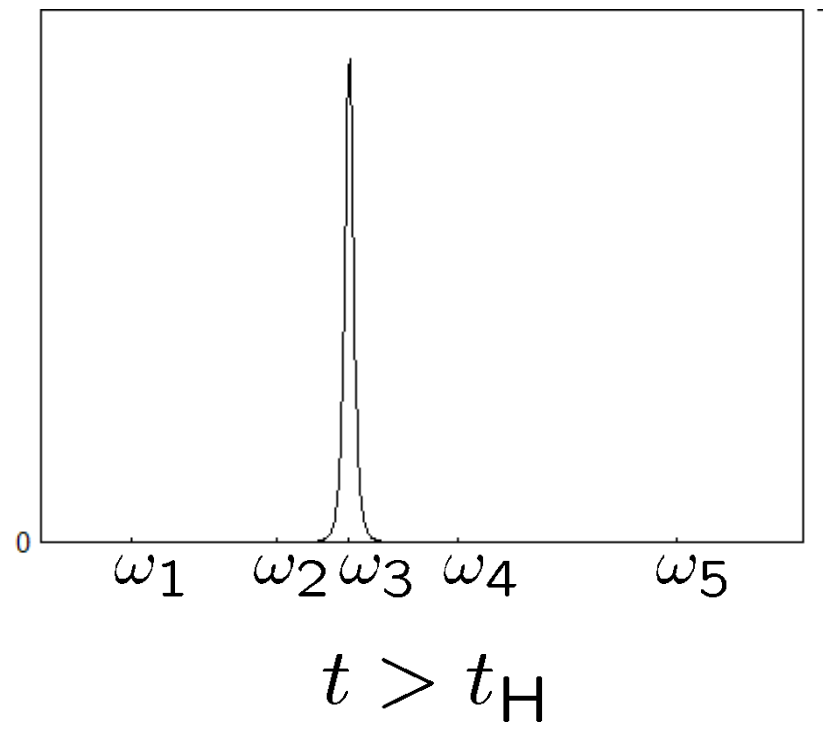


Only the narrowest mode survives in both cases

Long-time dynamics identical ?

# Breakdown of the theory for $t > t_{\mathrm{H}}$
# Path picture

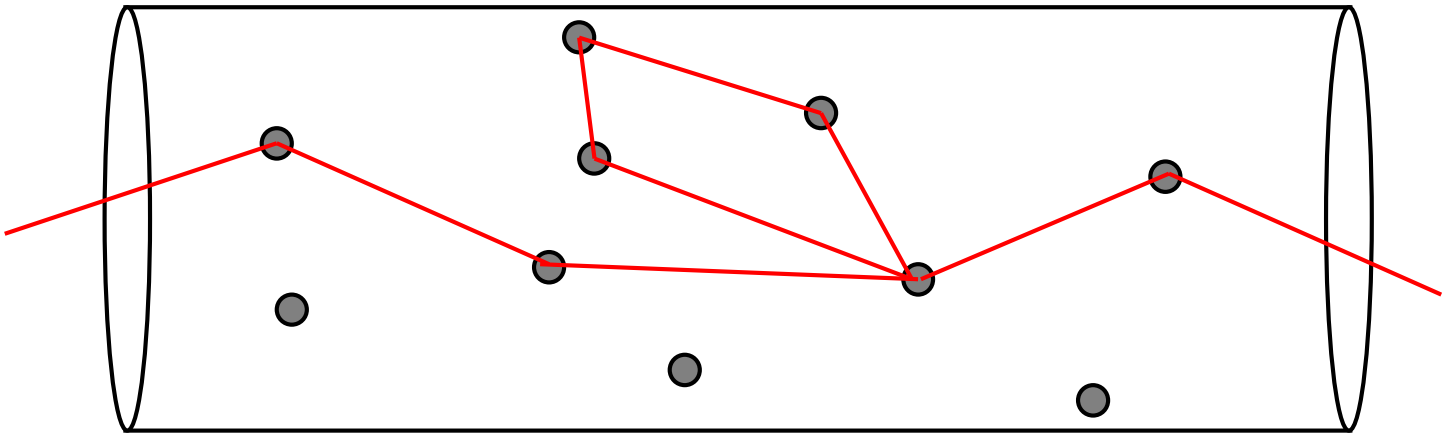

# Breakdown of the theory for $t > t_{\mathrm{H}}$
# Path picture

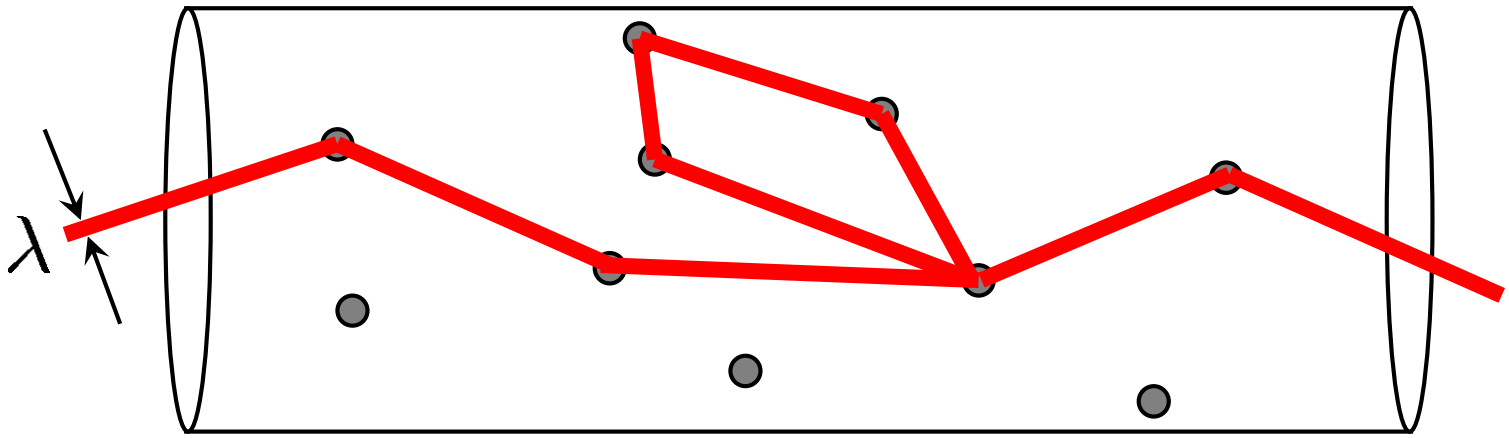


'Coherent' volume $= \lambda^3$

Number of coherent volumes $= \dfrac{\text{Volume}}{\lambda^3}$

Time needed to visit all coherent volumes $\sim t_{\mathrm{H}}$

For $t > t_{\mathrm{H}}$ any path will cross itself with probability 1

('return probability' $= 1$, as in 1D)

# Beyond the Heisenberg time

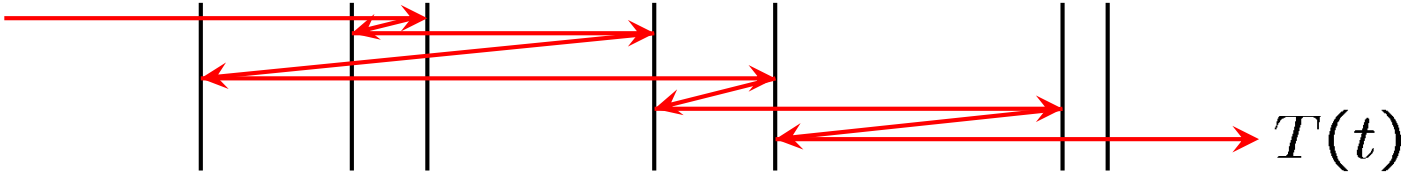


Randomly placed screens with random transmission coefficients

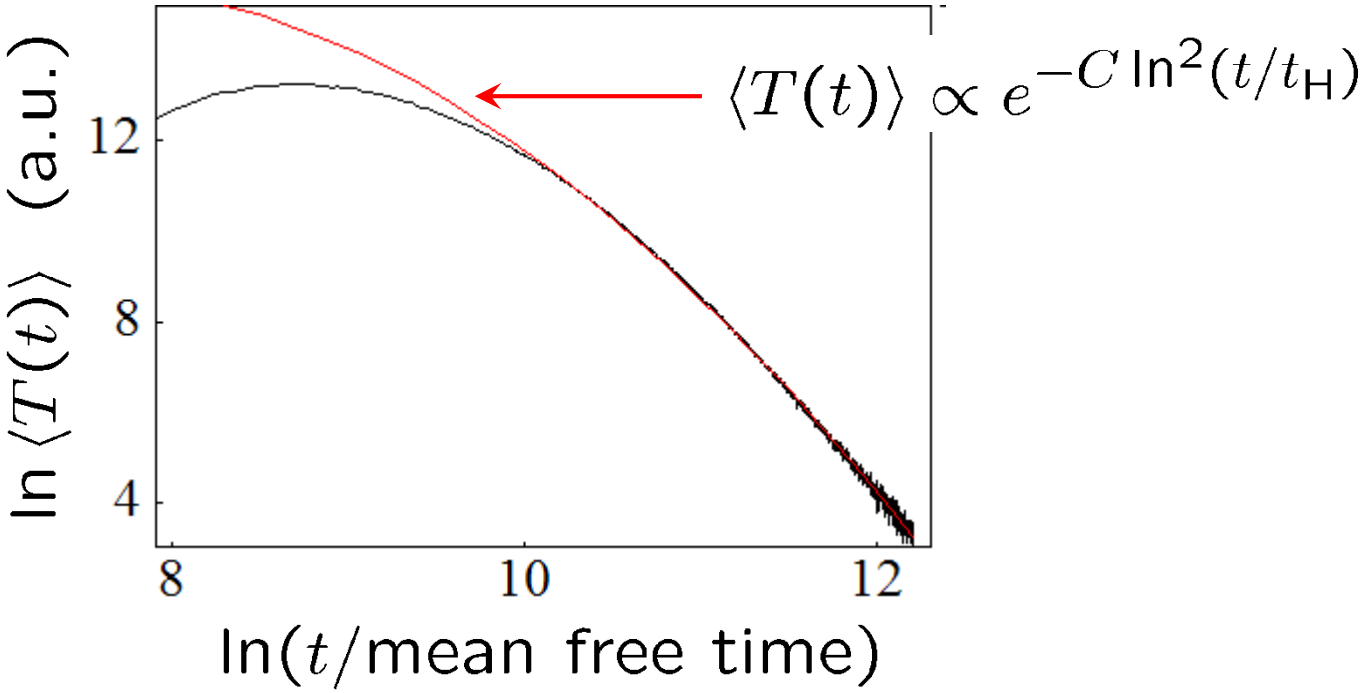

# Time-dependent reflection

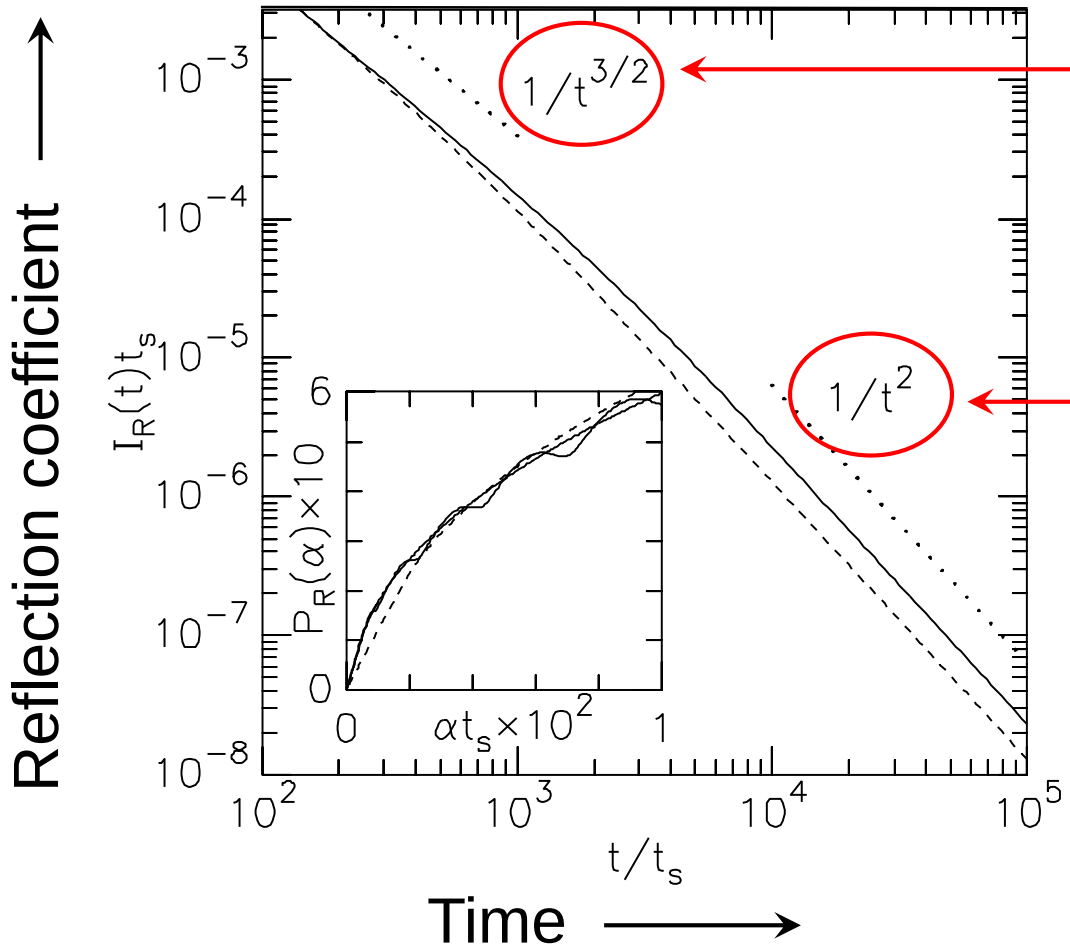


'Normal' diffusion

Localization

$N = 10$

$N = 20$

$L \gg \xi \gg \ell$

$t_H \to \infty$

Consistent with RMT result: M. Titov and C.W.J. Beenakker, *PRL* **85,** 3388 (2000) and 1D result ($N = 1$): B. White *et al. PRL* **59,** 1918 (1987)

# Generalization to higher dimensions

- Our approach remains valid in 2D and 3D
- For $t_{\mathsf{D}} < t < t_{\mathsf{H}}$ and $\ell \gg \lambda$ we get

$$\boxed{\frac{D(t)}{D_{\mathsf{B}}} = 1 + A\frac{t_{\mathsf{D}}}{t_{\mathsf{H}}} - B\frac{t}{t_{\mathsf{H}}}}$$

- $t_{\mathsf{H}} = \langle \Delta \rangle^{-1} = \mathsf{DOS} \times \mathsf{Volume}$

$$\mathsf{DOS} = \frac{k}{2\pi v_{\mathsf{E}}}\ (2\mathsf{D}), \quad \frac{k^2}{2\pi^2 v_{\mathsf{E}}}\ (3\mathsf{D})$$

Consistent with numerical simulations in 2D:
M. Haney and R. Snieder, *PRL* **91,** 093902 (2003)

# Conclusions

- Dynamics of multiple-scattered waves in quasi-1D disordered media can be described by a self-consistent diffusion model up to $t = t_{\mathsf{H}}$

- For $t_{\mathsf{D}} < t < t_{\mathsf{H}}$ and $\ell \gg \lambda$ we find a linear decrease of the time-dependent diffusion constant with $t/t_{\mathsf{H}}$ in *any dimension*

- Our results are consistent with recent microwave experiments, supersymmetric nonlinear $\sigma$-model, random matrix theory, and numerical simulations

HOP!

Application 1

# Tuning the conductance of single-walled carbon nanotubes by ion irradiation in the Anderson localization regime

C. GÓMEZ-NAVARRO[1], P. J. DE PABLO[1], J. GÓMEZ-HERRERO[1*], B. BIEL[2], F. J. GARCIA-VIDAL[2], A. RUBIO[3] AND F. FLORES[2]

[1]Departamento de Física de la Materia Condensada, Universidad Autónoma de Madrid, E-28049 Madrid, Spain

[2]Departamento de Física Teórica de la Materia Condensada, Universidad Autónoma de Madrid, E-28049 Madrid, Spain

[3]Departamento de Física de Materiales, Universidad del País Vasco UPV/EHU and Donostia International Physics Center (DIPC), E-20018-San Sebastián, Spain

*e-mail: julio.gomez@uam.es

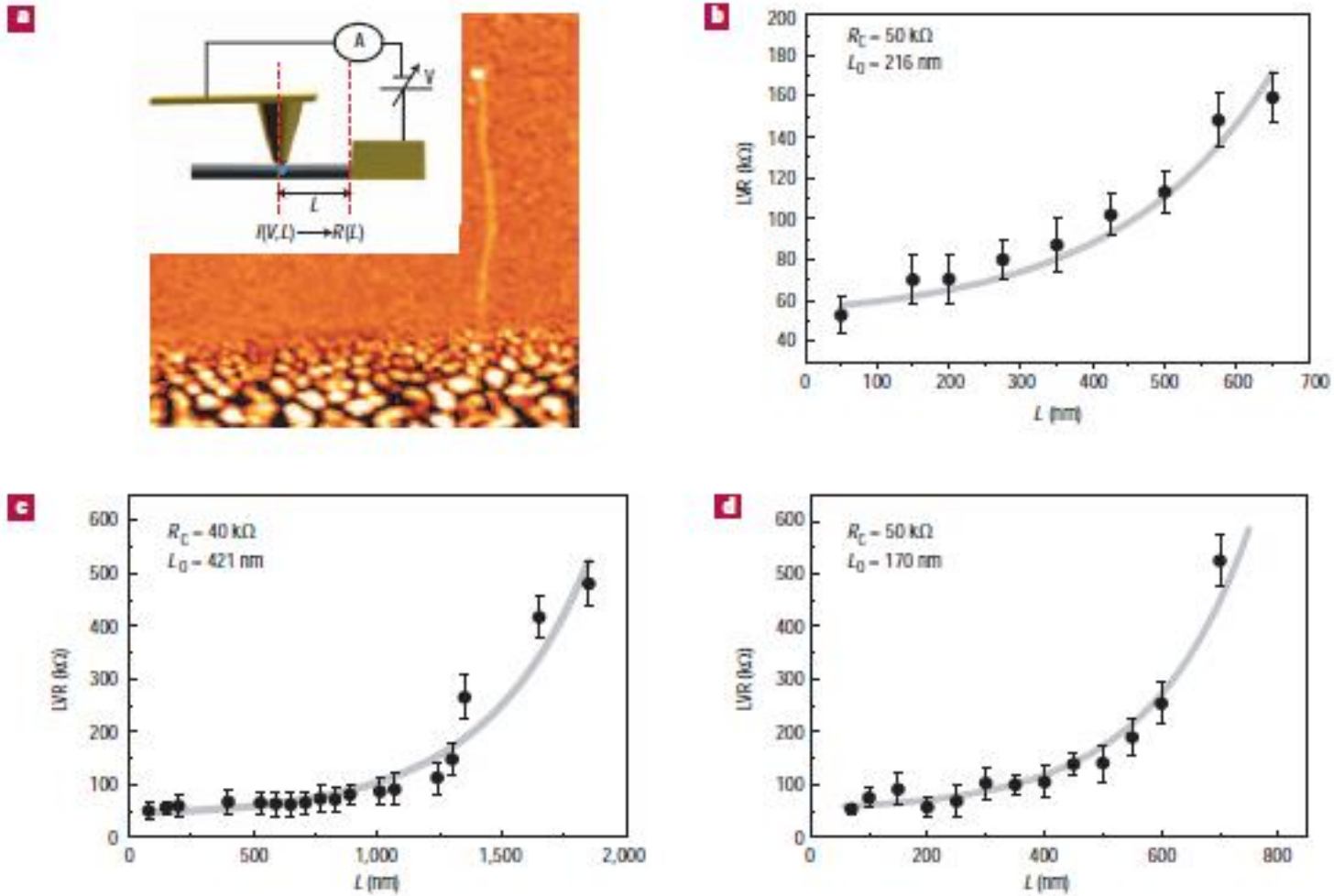


**Figure 1 Experimental setup. a**, AFM image (1 μm × 1 μm) of an SWNT adsorbed on an insulating substrate connected to a gold electrode (bottom). The inset is a scheme of the experimental setup showing a gold-covered AFM tip, the macroscopic gold electrode, the SWNT and the circuit used. **b–d**, Plots of the LVR versus length for three metallic SWNTs as deposited on the surface, without irradiation. The data are fitted to equation (1). The values of $R_c$ and $L_0$ obtained for the best fit are depicted in each chart. The error bars represent one standard deviation. **[Author: OK?]** Data for the nanotube in **b** after irradiation are presented in Fig. 2.

$$R(L) = R_c + 1/2R_0\exp(L/L_0)$$

where $R_c$ is the contact resistance, $R_0$ is the inverse of the quantum of conductance $G_0 = 2e^2/h$ (where $e$ is the charge on the electron and h is Planck's constant;[**Author: OK?**] the 1/2 factor in equation (1) accounts for the two conductance channels of a metallic SWNT, see below) and $L_0$ is the localization length. The exponential resistance

Application 2

# Electrical transport in granular metals
# Variable range hopping

**Variable-range hopping** is a model used to describe carrier transport in disordered systems by hopping through localized states in an extended temperature range. It has a characteristic temperature dependence of

$$\sigma = \sigma_0 e^{-(T_0/T)^\beta}$$

where $\beta$ is a parameter dependent on the model under consideration.

**Hopping mechanism is a term coined to denote the combination of thermal activation and tunneling. Thermal activation and tunneling, nominally independent, can actually couple to give**

$$\sigma = \sigma_0 e^{-(T_0/T)^\beta}$$

**HOPPING=TUNNELLING+THERMAL ACTIVATED TRANSPORT**

Granular metals are composites consisting of a random mixture of nanometer-sized metal and insulator grains. As a function of metal volume fraction, the structure and electrical properties of the granular metals can be divided into two regimes, separated by the percolation threshold. In the metal-rich regime, metal grains form a connected network, and electrical conduction is by electron percolation through the metallic channels. In the insulator-rich regimes, metal grains are dispersed in the matrix of the insulator. In this dielectric regime the electrical transport is via the hopping mechanism.

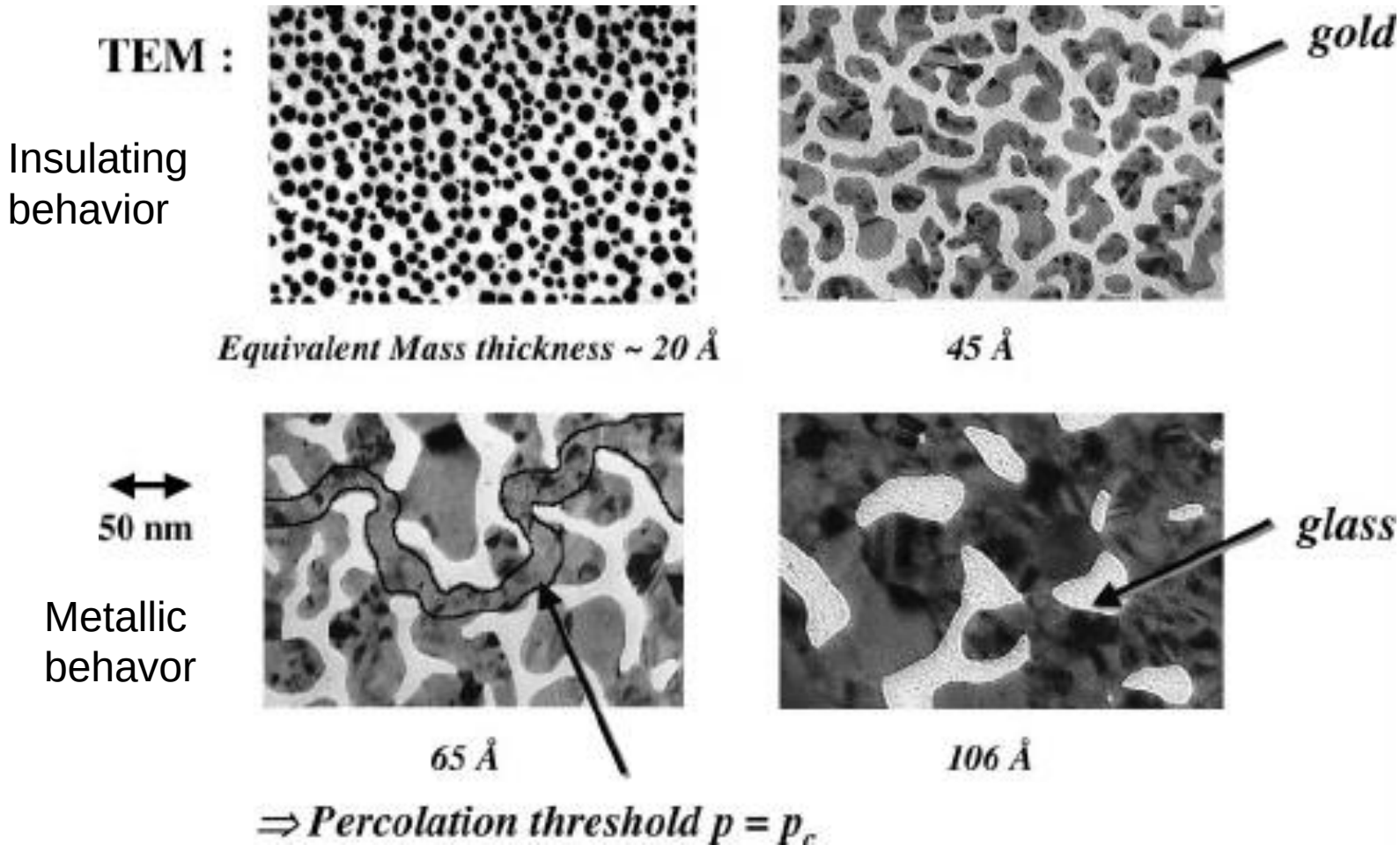

PHYSICAL REVIEW B **78**, 165418 (2008)

# Percolation in nanoporous gold and the principle of universality for two-dimensional to hyperdimensional networks

G. B. Smith, A. I. Maaroof, and M. B. Cortie

*Department of Physics and Advanced Materials and Institute for Nanoscale Technology, University of Technology, Sydney, P.O. Box 123, Broadway, New South Wales 2007, Australia*

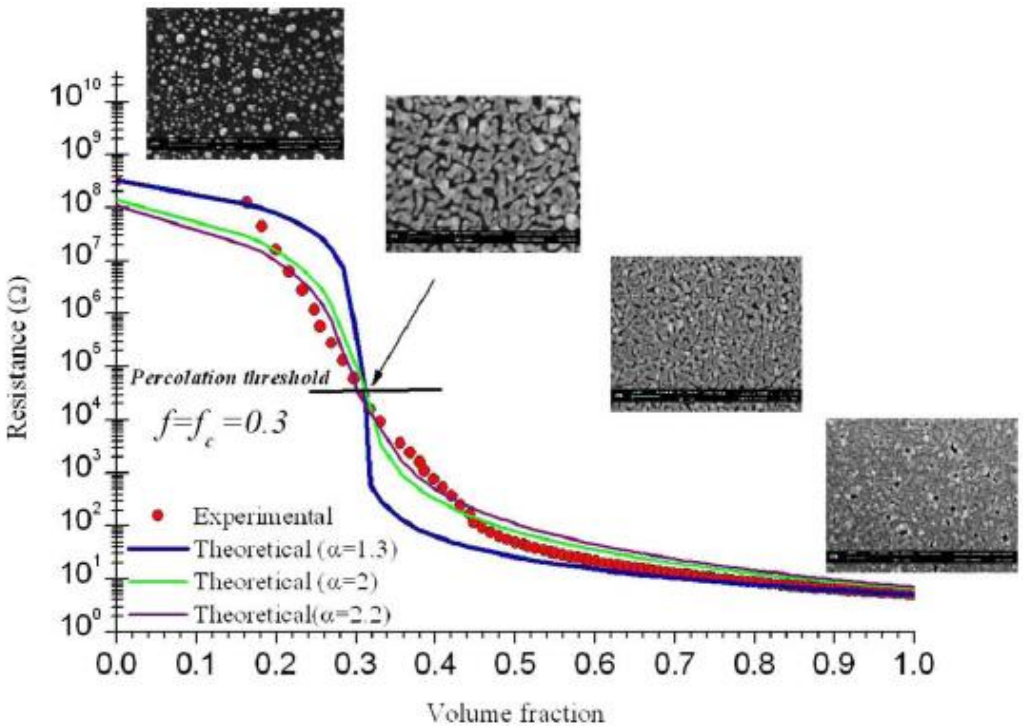


FIG. 3. (Color online) Resistance of a growing gold film on glass as a function of volume (or area) fraction $f$ of gold. Images included show characteristic morphology at each stage of gold coverage. Models for $d=2$ and $d=3$ percolation are included, along with a critical curve for $\alpha=2.2$.

$$R = A(f - f_c)^{-\alpha_+}, \quad f > f_c,$$

$$R = B(f_c - f)^{\alpha_-}, \quad f < f_c.$$

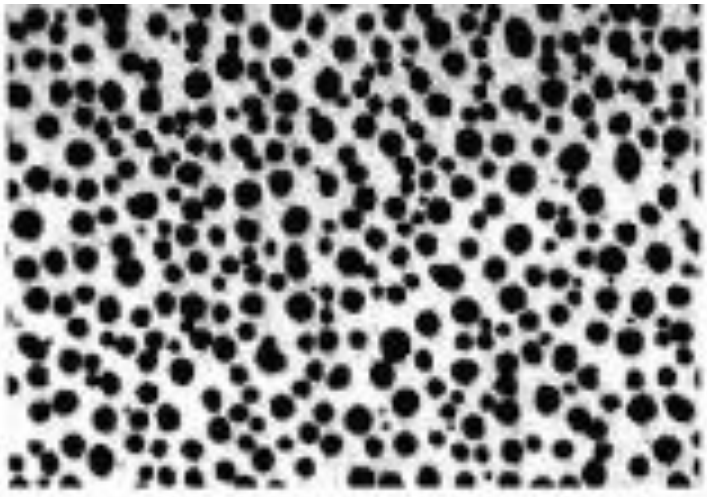

## Mott variable-range hopping [ edit ]

The **Mott variable-range hopping** describes low-temperature conduction in strongly disordered systems with localized charge-carrier states[2] and has a characteristic temperature dependence of

$$\sigma = \sigma_0 e^{-(T_0/T)^{1/4}}$$

for three-dimensional conductance (with $\beta$ = 1/4), and is generalized to *d*-dimensions

$$\sigma = \sigma_0 e^{-(T_0/T)^{1/(d+1)}}.$$

## Efros–Shklovskii variable-range hopping [ edit ]

*See also: Coulomb gap*

The **Efros–Shklovskii (ES) variable-range hopping** is a conduction model which accounts for the Coulomb gap, a small jump in the density of states near the Fermi level due to interactions between localized electrons.[5] It was named after Alexei L. Efros and Boris Shklovskii who proposed it in 1975.[5]

The consideration of the Coulomb gap changes the temperature dependence to

$$\sigma = \sigma_0 e^{-(T_0/T)^{1/2}}$$

for all dimensions (i.e. $\beta$ = 1/2).[6][7]

# Variable-range hopping

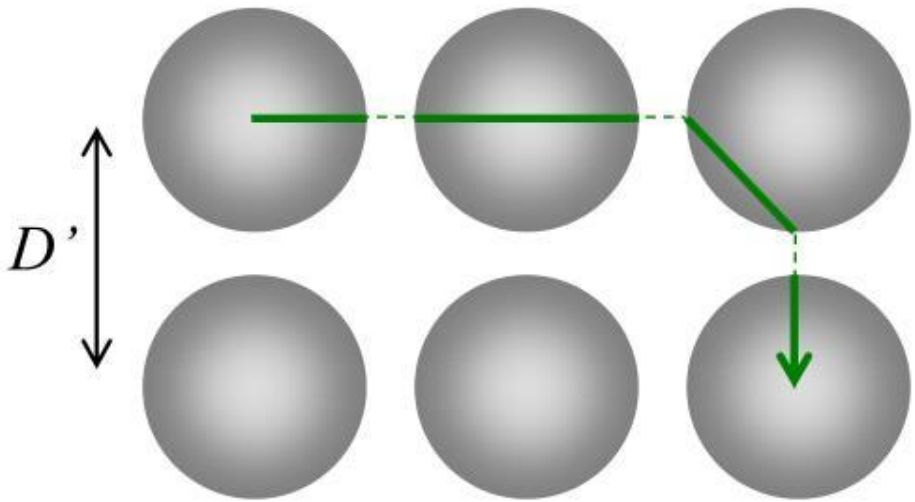


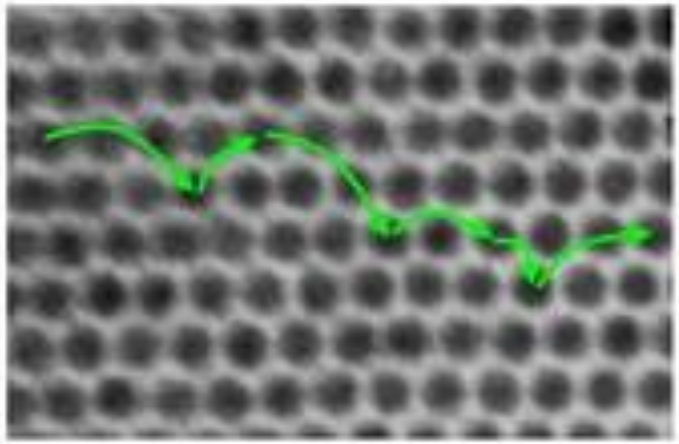

rate of phonon-assisted tunneling:

$$\Gamma \propto \exp\left[-\frac{2r}{\xi} - \frac{\Delta E}{k_B T}\right]$$

$\xi$ = localization length

$$\xi \sim a\, D'/d >> a$$

# Electron conduction in NC arrays

Download

Conventional hopping models:

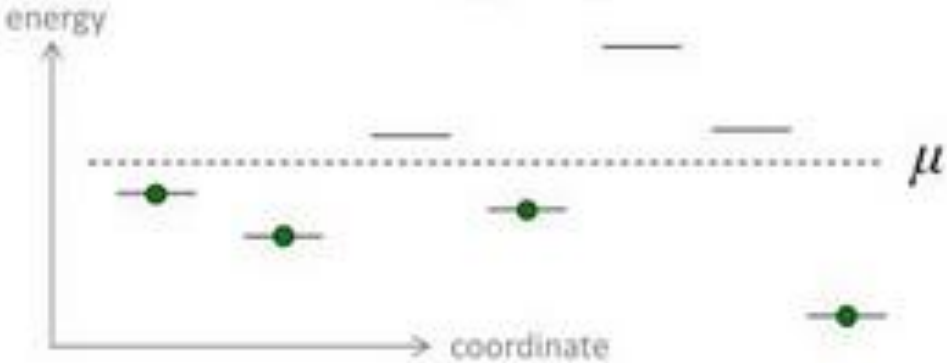


**Each site has one energy level: filled or empty.**

Conductivity is tuned by:

- spacing between sites
- insulating material
- disorder in energy/coordinate
- Fermi level $\mu$

In nanocrystal arrays:

**Each "site" is a NC, with a spectrum of levels:**

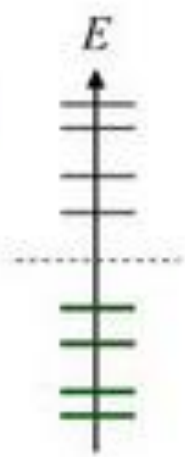


Energy level spectrum is tailored by:

- size
- composition
- shape
- surface chemistry
- magnetism
- superconductivity
- etc.

# Electron conduction in NC arrays

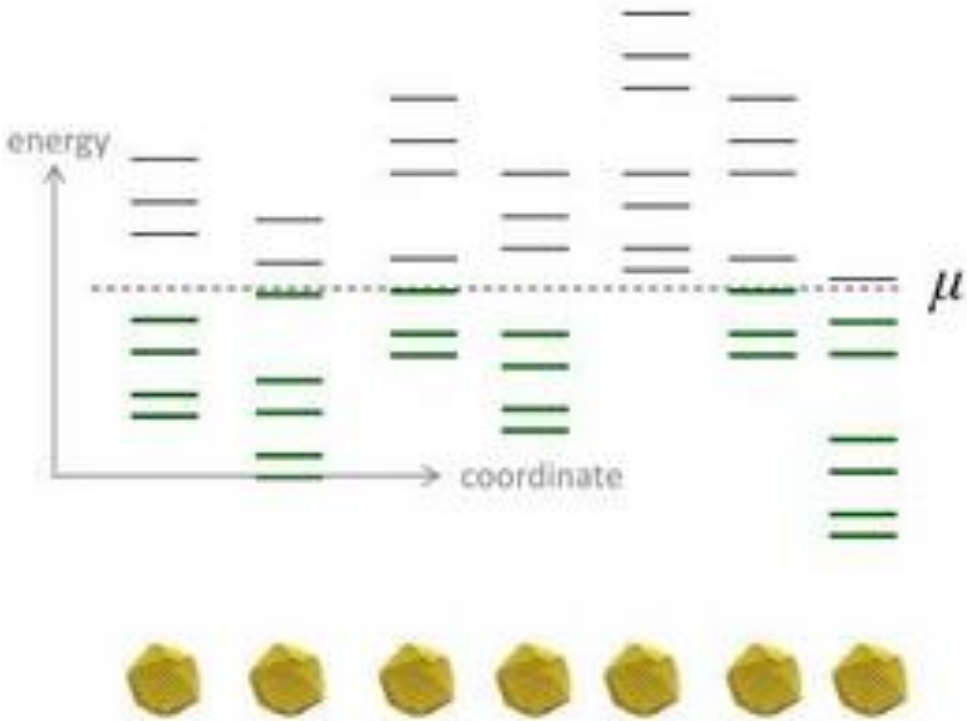


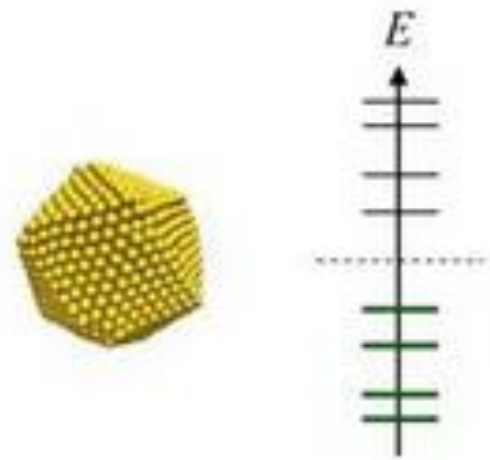


Conductivity reflects the interplay between individual energy level spectrum and global, correlated properties.

# Experiment: metallic NCs

precise control over size/spacing:

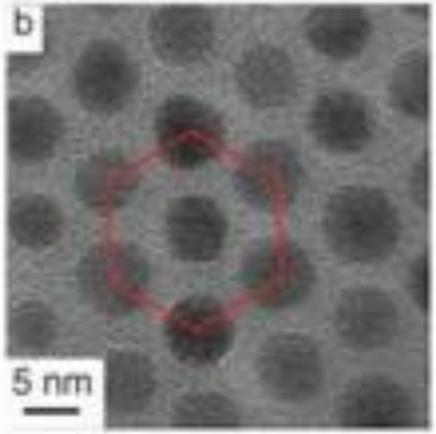


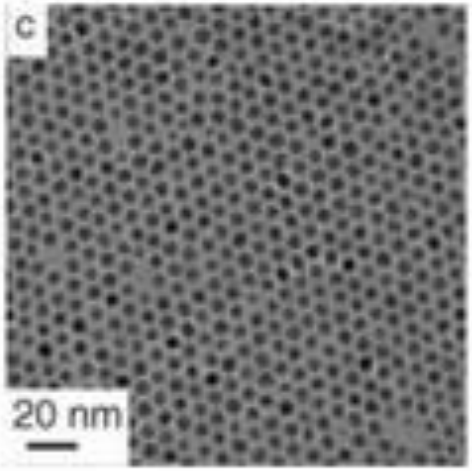


[Aubin group, ESPCI ParisTech]

tuneable metal/insulator transition:

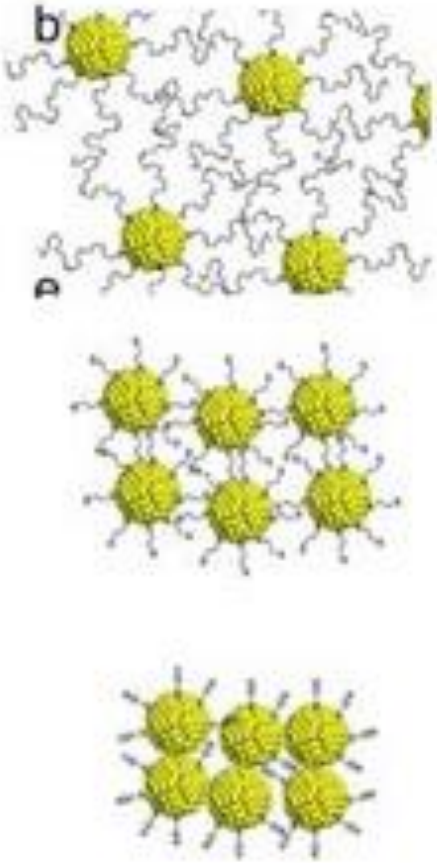


[Kagan and Murray groups, UPenn]

range of shapes:

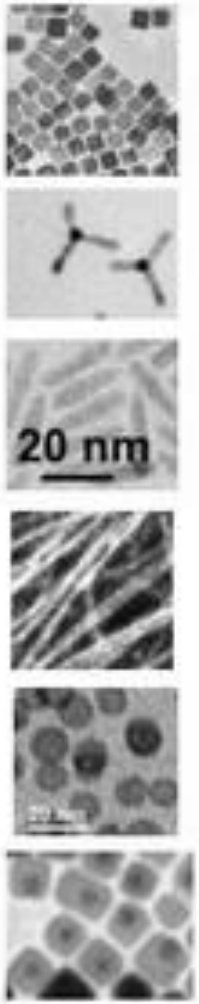


cubes

stars

rods

wires

hollow spheres

core/ shell

[Talapin group, Chicago]

# Model of an array of metal NCs

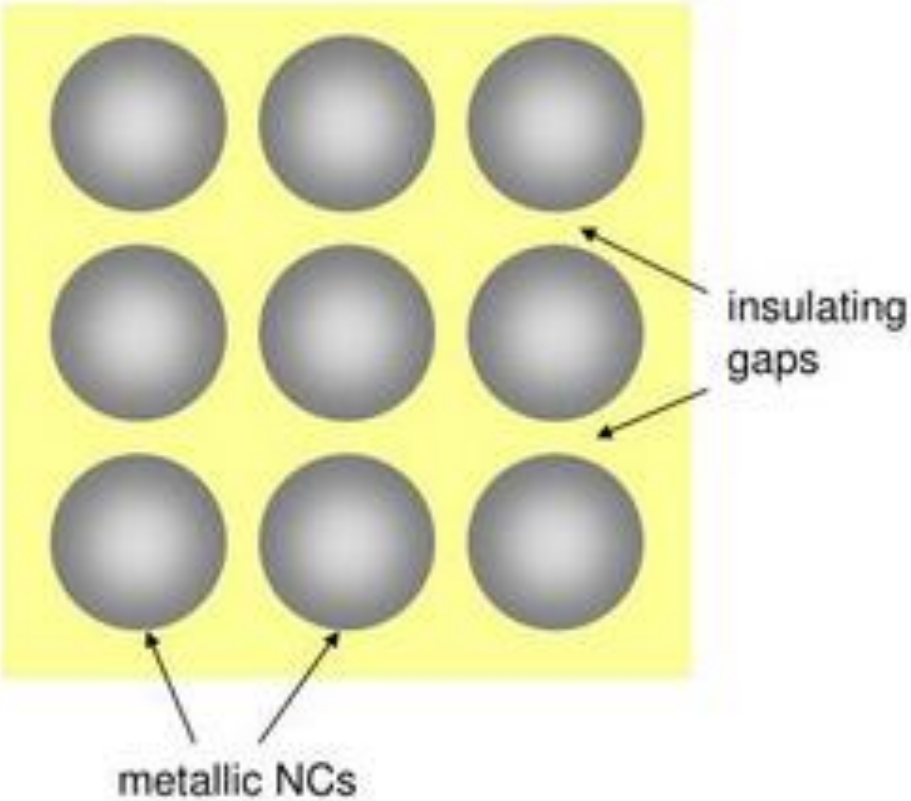


Uniform, spherical, regularly-spaced metallic NCs with insulating gaps

Large internal density of states: spacing between quantum levels

$\delta \rightarrow 0$

# Model of an array of metal NCs

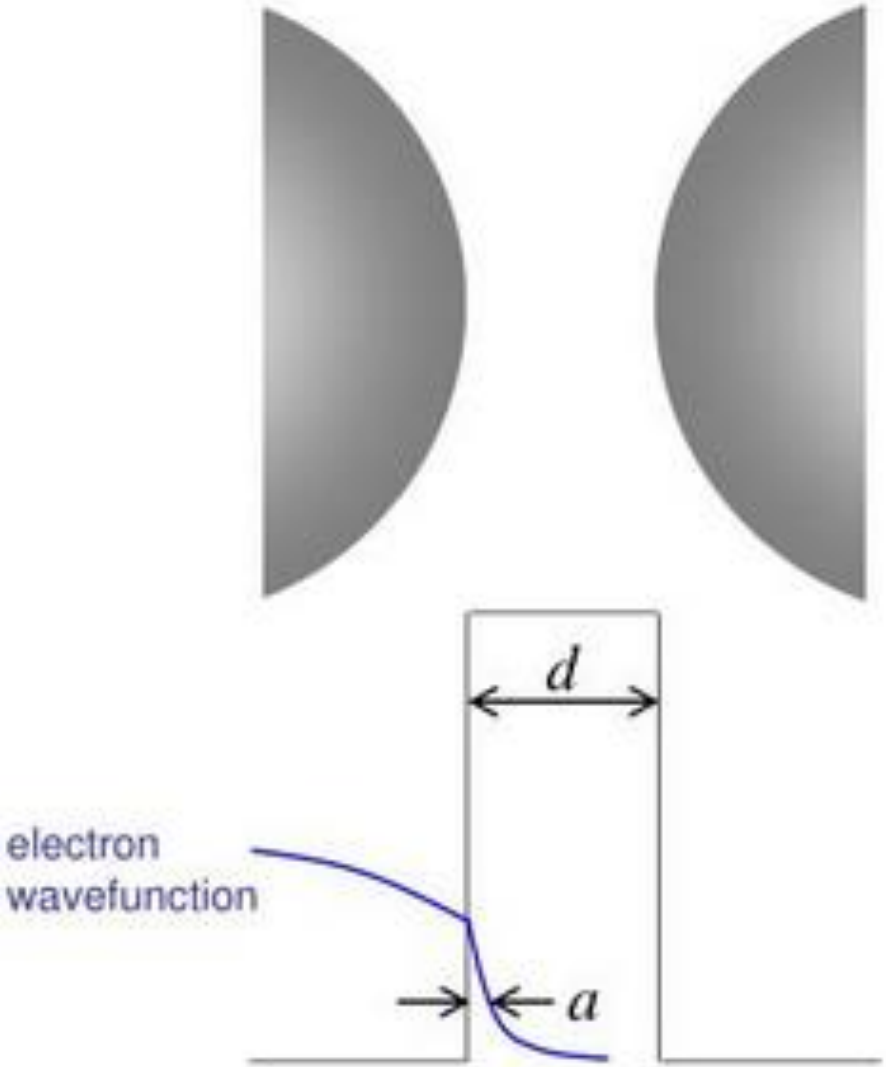


High tunneling barriers

$a << d$

Tunneling between NCs is weak:

$G/(e^2/h) << 1$

# Single-NC energy spectrum

Download

A single, isolated NC:

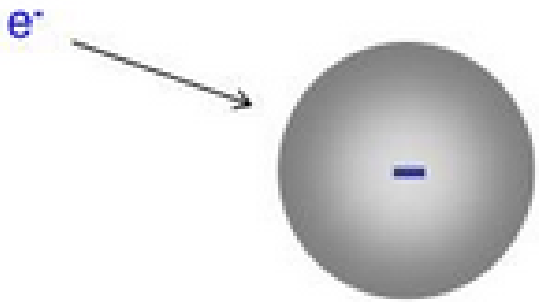


Coulomb self-energy:

$$E_c = e^2/2C_0$$

ground state energy levels:

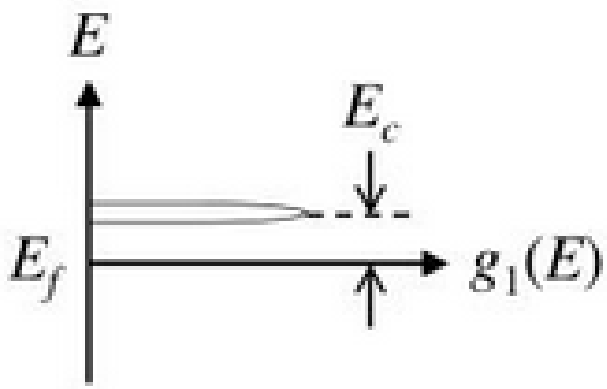

# Single-NC energy spectrum

Download

Multiple-charging:

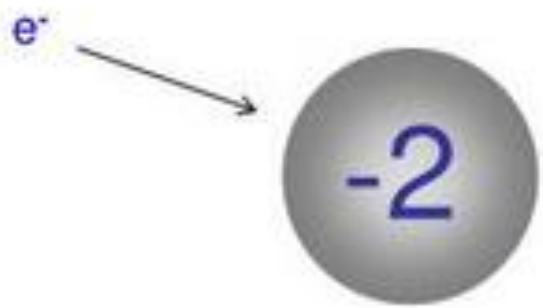


Coulomb self-energy:

$$E_c = e^2/2C_0$$

$$\rightarrow (2e)^2/2C_0$$

ground state energy levels:

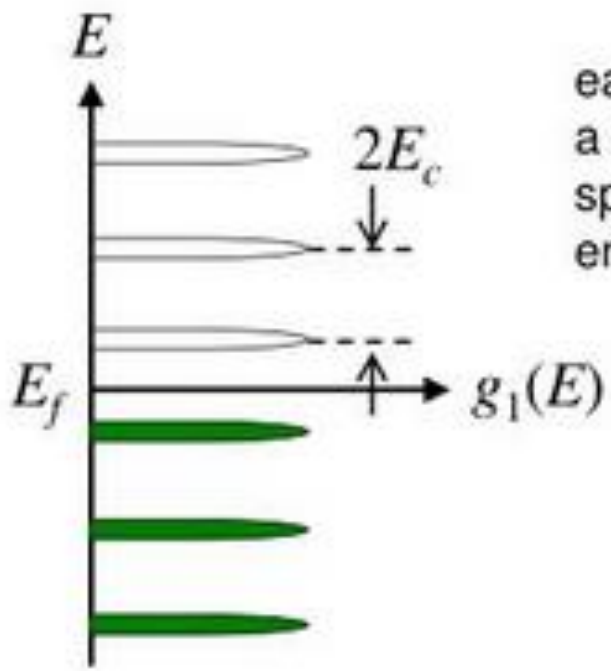


each NC has a periodic spectrum of energy levels

**Same spectrum that gives rise to the Coulomb blockade**

# Density of Ground States

Disorder randomly shifts NC energies:

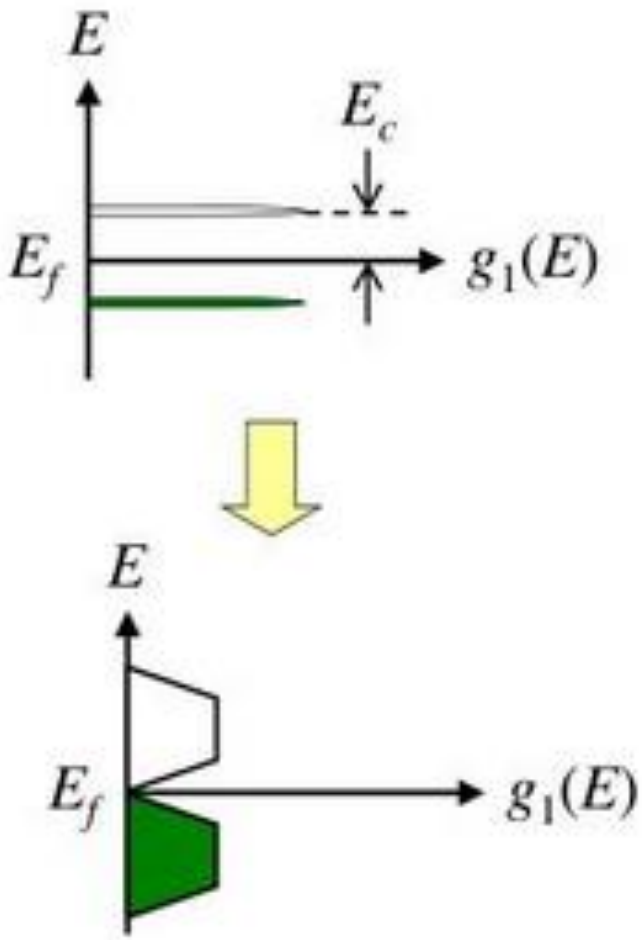


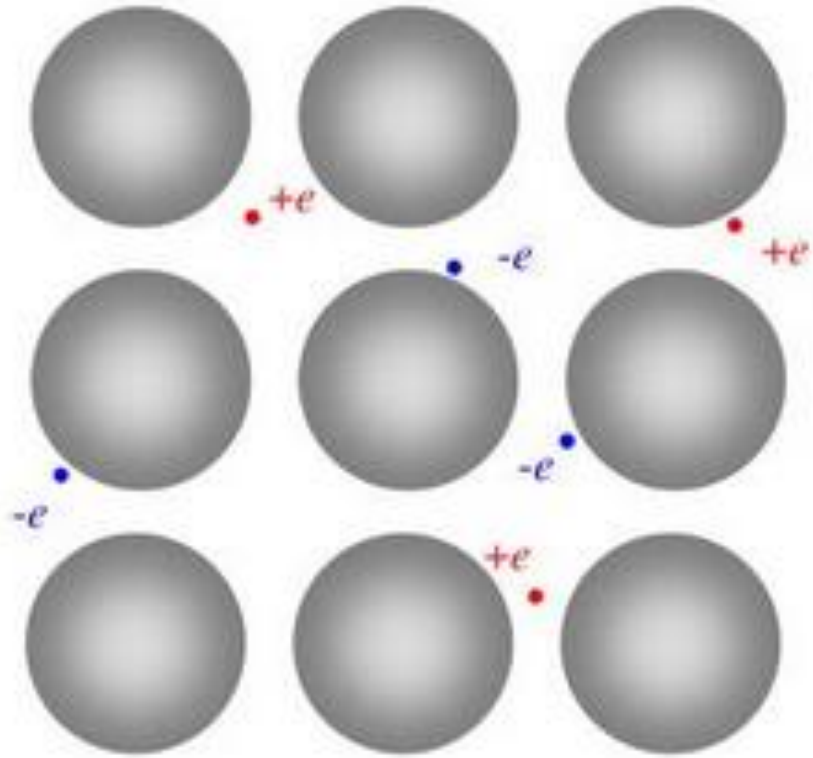


"Density of ground states" (DOGS): distribution of lowest empty and highest filled energies across all NCs

# The Coulomb gap


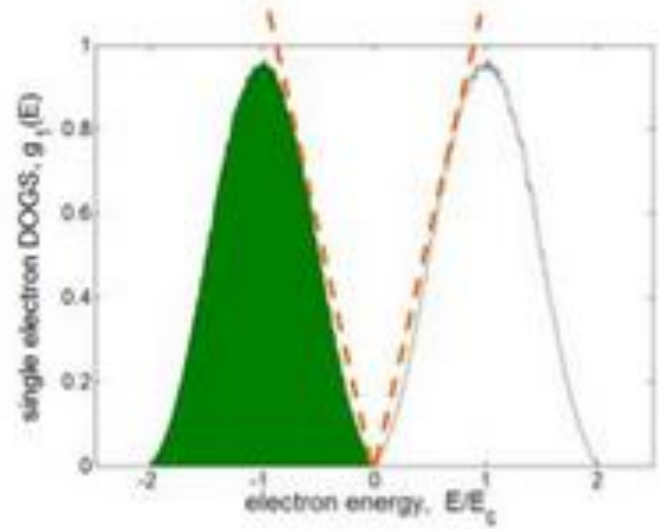


$$E^- - \left(E^+ - \frac{e^2}{\kappa r}\right) > 0 \Rightarrow E^+ - E^- > \frac{e^2}{\kappa r}$$

$$g(E) \lesssim \frac{|E|}{\kappa e^4} \quad \text{in 2D}$$

Efros-Shklovskii conductivity:

$$\rho \propto \exp\left[\left(\frac{T_{ES}}{T}\right)^{1/2}\right]$$

Typical hop length:

$$r_{\text{hop}} \sim \left(\frac{4\pi\varepsilon\xi}{e^2 k_B T}\right)^{1/2}$$

# Variable-range hopping

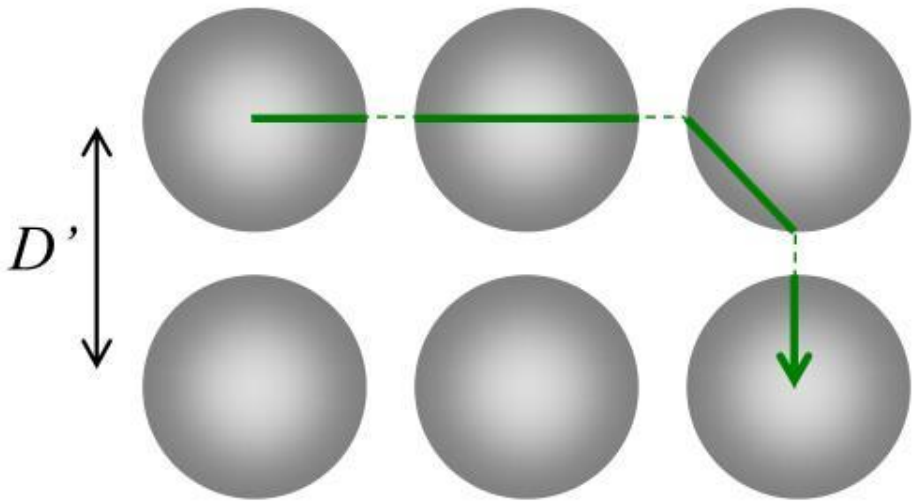


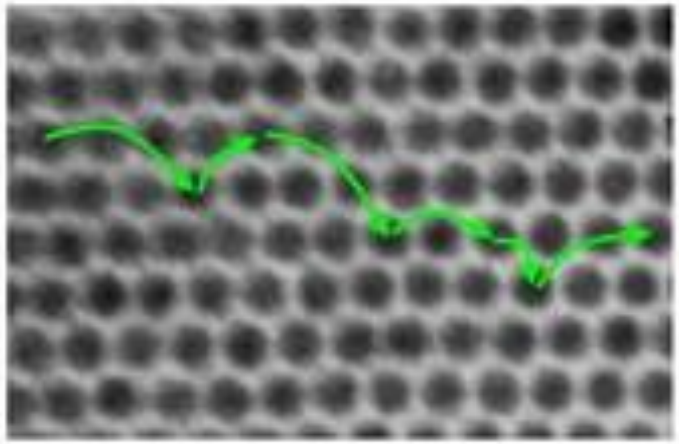

rate of phonon-assisted tunneling:

$$\Gamma \propto \exp\left[-\frac{2r}{\xi} - \frac{\Delta E}{k_B T}\right]$$

$\xi$ = localization length

$$\xi \sim a\, D'/d >> a$$

# Variable-range hopping

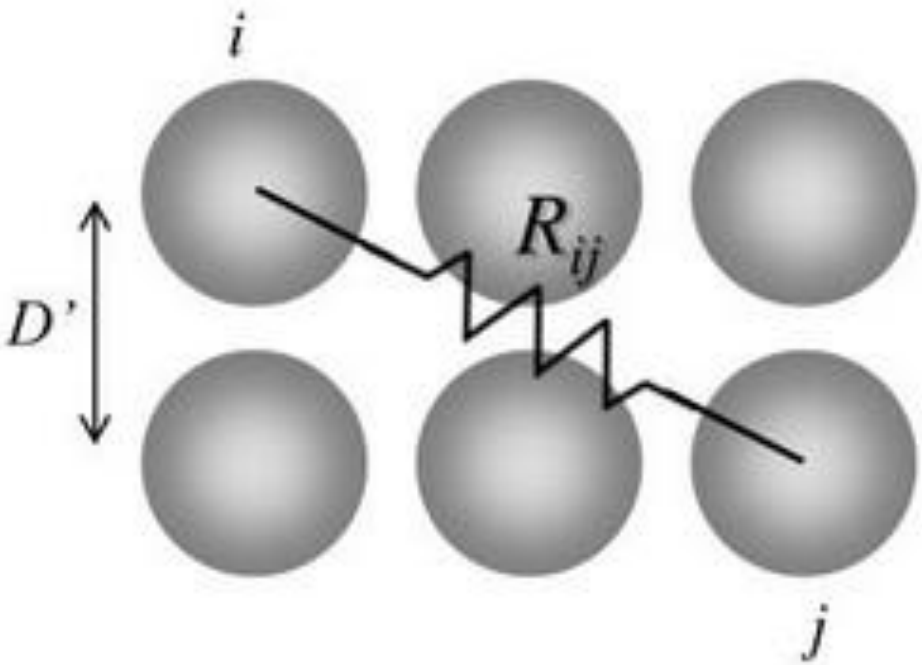


$$R_{ij} \propto \exp\left[\frac{2r}{\xi} + \frac{\Delta E_{ij}}{k_B T}\right]$$

rate of phonon-assisted tunneling:

$$\Gamma \propto \exp\left[-\frac{2r}{\xi} - \frac{\Delta E}{k_B T}\right]$$

$\xi$ = localization length

# Efros-Shklovskii conductivity

Download

$$\rho \propto \exp\left[\left(\frac{T_{ES}}{T}\right)^{1/2}\right]$$

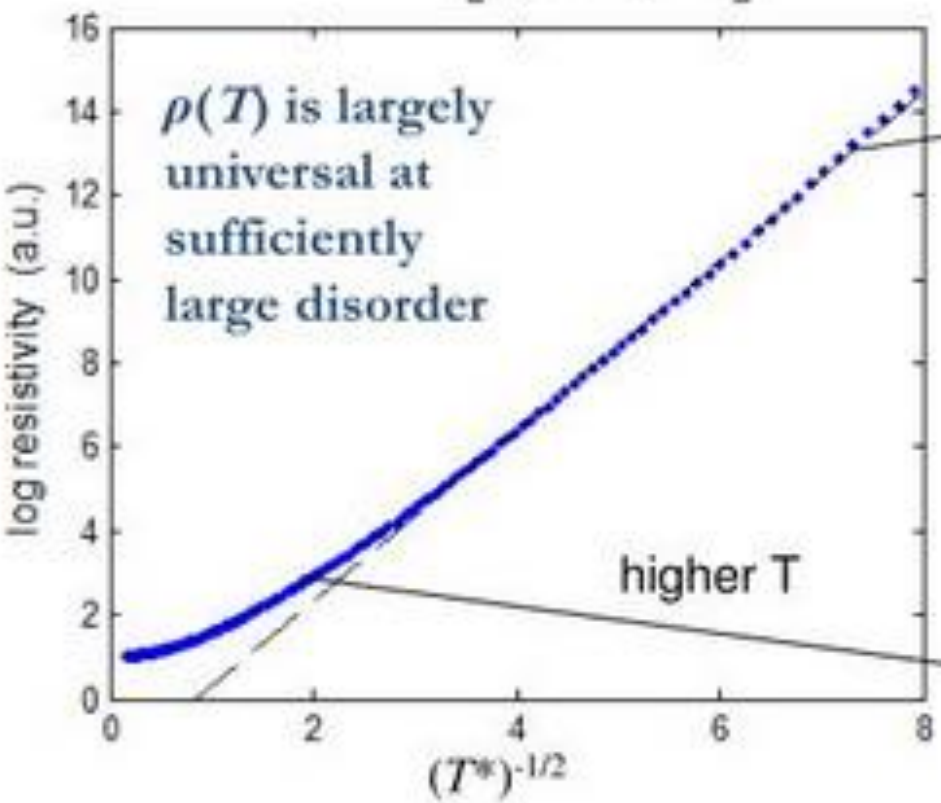


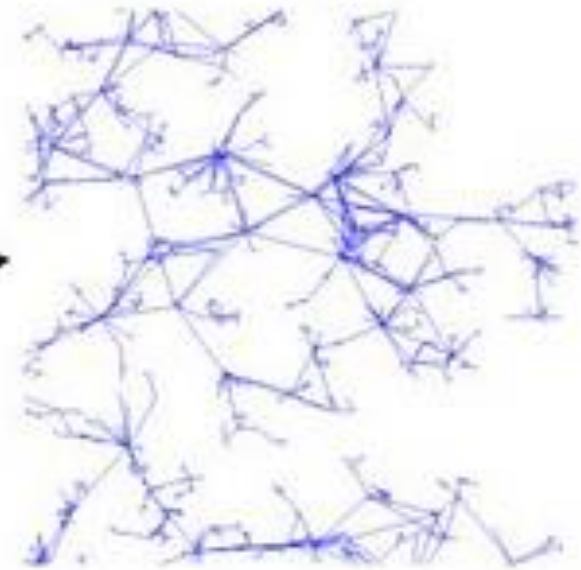

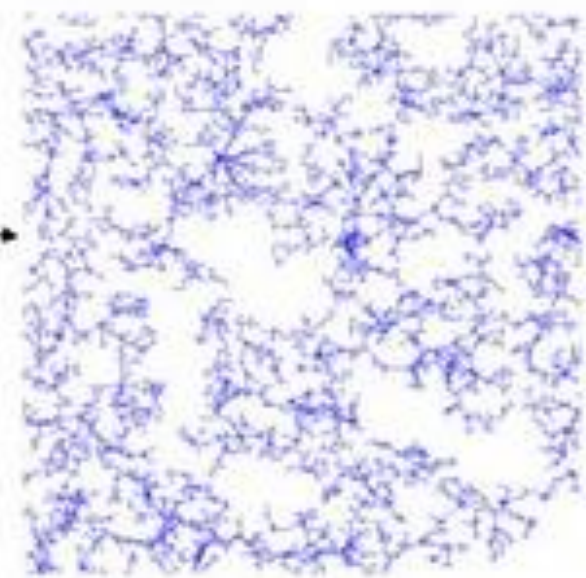

$$T^* = \frac{2Dk_BT}{E_c\xi}$$

# Temperature-Dependent Electron Transport through Silver Nanocrystal Superlattices

**R. Christopher Doty,[†] Hongbin Yu,[‡] C. Ken Shih,[‡] and Brian A. Korgel*[,†]**

*Department of Chemical Engineering and Texas Materials Institute, Center for Nano- and Molecular Science and Technology, University of Texas, Austin, Texas 78712-1062, and Department of Physics and Texas Materials Institute, Center for Nano- and Molecular Science and Technology, University of Texas, Austin, Texas 78712-1062*

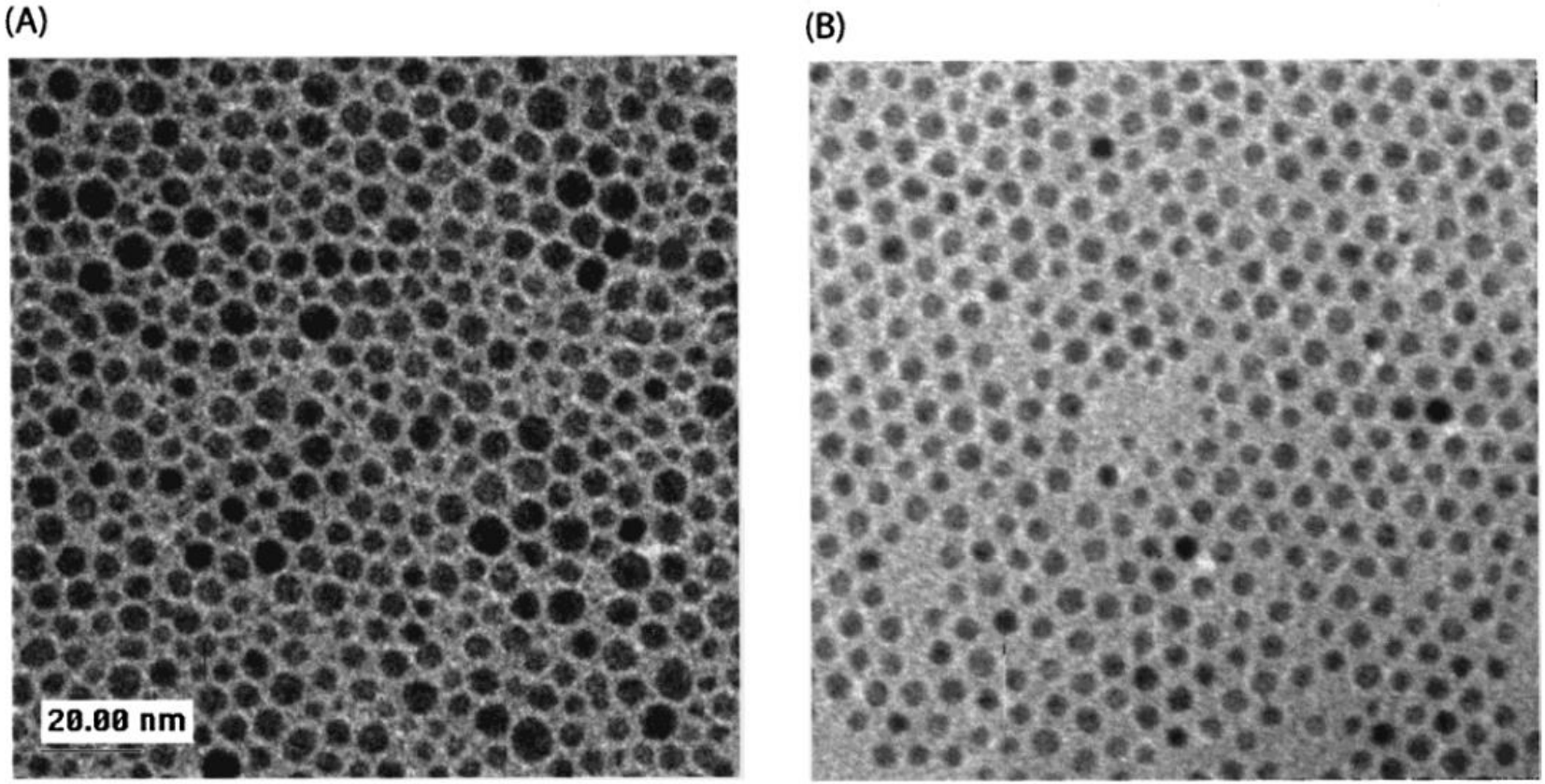


**Figure 2.** TEM images of (A) size-polydisperse (3.8 ± 0.8 nm) dodecanethiol-capped silver nanocrystals and (B) size-monodisperse (3.7 ± 0.3 nm) dodecanethiol-capped silver nanocrystals.

A Mott transition is a metal-nonmetal transition in condensed matter.

A Mott Transition is a change in a material's behavior from insulating to metallic due to various factors.

The physical origin of the Mott transition is the interplay between the Coulomb repulsion of electrons and their degree of localization (band width). Once the carrier density becomes too high, the energy of the system can be lowered by the localization of the formerly conducting electrons (band width reduction), leading to the formation of a band gap.

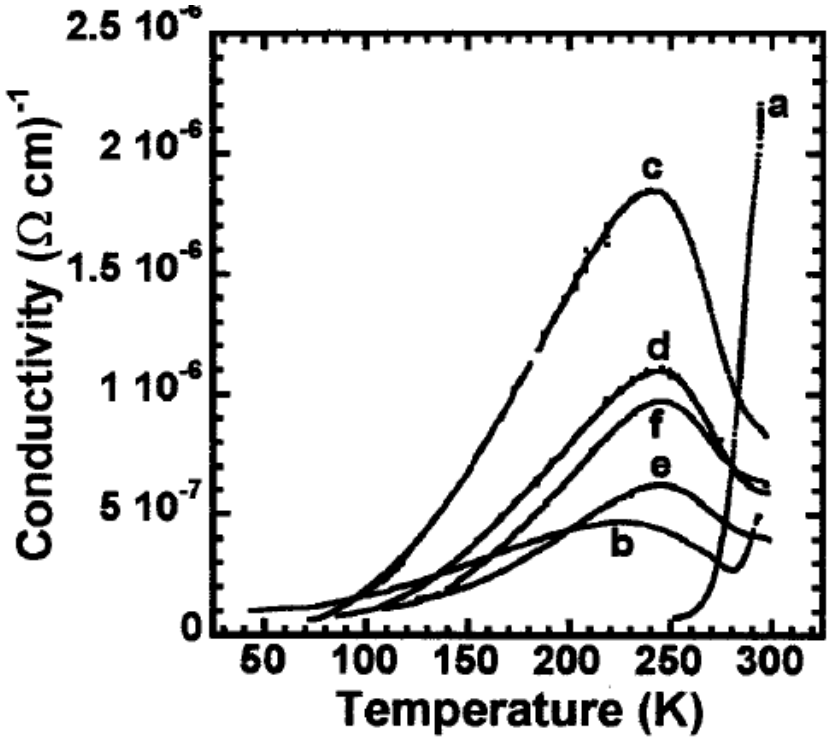


**Figure 5.** Conductivity versus temperature data for silver nanocrystal films: (a) size-polydisperse sample; size-monodisperse samples with diameters of (b) 7.7 nm; (c) 5.5; (d) 4.8; (e) 4.5; (f) 3.5.

**TABLE 1: Parameters**

| nanocrystals | diameter (nm) | $T_{MI}$ (K) | $\sigma$ at $T_{MI}$ ($10^{-6}\,\Omega^{1-}$) | $T_o$ (K) | conductance exponent, $\upsilon$ | activation energy, $E_g$ (eV) |
|---|---|---|---|---|---|---|
| polydisperse sample (a) | | | | | | 1.5 |
| fraction 1 (b) | 7.7 | 225 | 0.47 | 500 | 0.67 | 0.038 |
| fraction 2 (c) | 5.5 | 241 | 1.8 | 300 | 1.22 | 0.069 |
| fraction 3 (d) | 4.8 | 244.5 | 1.1 | 300 | 1.34 | 0.079 |
| fraction 4 (e) | 4.2 | 245 | 0.63 | 325 | 1.35 | 0.080 |
| fraction 5 (f) | 3.5 | 245 | 0.98 | 350 | 1.34 | 0.098 |

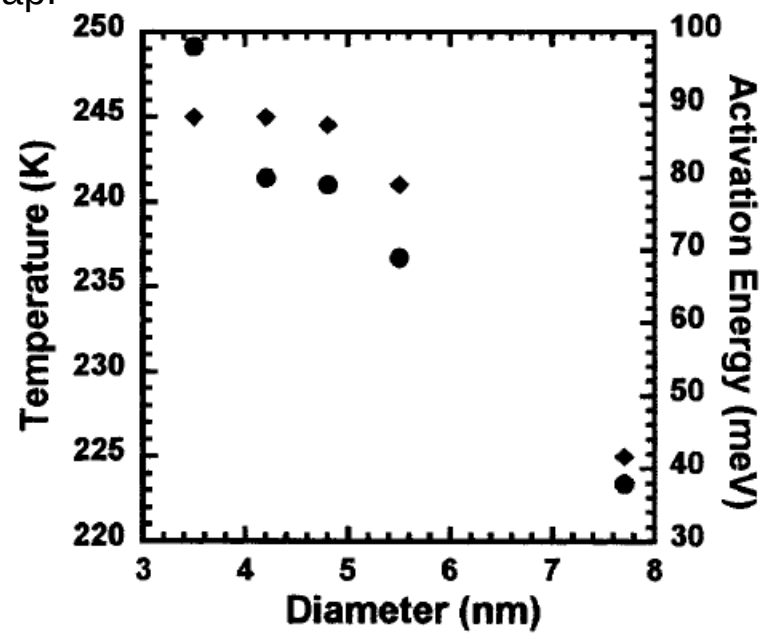


**Figure 6.** Plot of transition temperature ($T_{MI}$, ◆) and activation energy ($E_g$, ●) of dodecanethiol-capped silver nanocrystals as a function of particle diameter.